Design improvements to *in vitro* gastrointestinal models to evaluate effectiveness of insulin encapsulation in nanoparticles

by

Kaitlin E. Reilly

A thesis submitted to the Department of Chemical Engineering

In conformity with the requirements for

the degree of Master of Applied Science

Queen's University

Kingston, Ontario, Canada

(August, 2011)

Abstract

The goal of this study was to develop a model of the gastrointestinal tract (GIT) to be used for *in vitro* testing of oral insulin delivery devices. The method and intensity of mixing and effects of gastrointestinal fluids with and without enzymes were evaluated. Comparisons were made between an actively mixed simulator and a passively mixed simulator, where the actively mixed simulator is a magnetically stirred flask while the passively mixed simulator is a flexible container on a rocking stage. Slower mixing times and larger time constants for mixing were seen for the passively mixed simulator during a pH tracer experiment. Release studies were performed with several oral insulin delivery device models to evaluate the effects of different mixing techniques on insulin release. In all cases, the more intense mixing of the actively mixed simulator resulted in more insulin release. When using a nanoparticle model in intestinal fluid for example, 100% insulin release was observed in the actively mixed simulator while only 53% was released in the passively mixed simulator after 1 hour. Trypsin and pepsin were used to determine the ability of a drug delivery device to protect insulin from enzymatic degradation in which trypsin was added to simulated intestinal fluid and pepsin was added to simulated gastric fluid. Premature insulin release and insulin denaturation at body temperature occurred in the intestinal fluid so the protective effects against trypsin were unable to be effectively evaluated. An increase in insulin loss from 70% to 95% was detected in the presence of pepsin compared to gastric fluid without enzymes in the actively mixed simulator, indicating that acid hydrolysis of insulin as well as protease attack by pepsin will impact the behavior of an insulin delivery device. An improvement in insulin retention was observed in the passively mixed simulator. After 1 hour, insulin

retained was increased from 4% in the actively mixed simulator to 10% in the passively mixed simulator, and after 2 hours, this increase was 2% to 7%. Premature insulin release from the delivery device, acid hydrolysis, temperature denaturation, and enzymatic degradation are factors limiting the effectiveness of oral insulin.

Acknowledgments

First and foremost, I would like to extend my thanks to my supervisor Dr. Ronald Neufeld. His guidance through this process has encouraged me to grow and develop both professionally and personally. The skills I have gained here will allow me to be a better informed and more effective contributor in all of my future professional experiences.

Thank you to Matt Caicco for his help in both developing the gastrointestinal model and performing preliminary testing. His passion and dedication to high quality work has been invaluable to this project.

Thanks for the support from my lab mates, Michael Hyrnyk, Joe Steele, and Camile Woitiski. Thank you for sharing your knowledge, experiences, creativity, and most of all your friendship.

To my family, especially my mom and dad, who are always there to support and encourage me in every aspect of my life. Thank you for always believing in me and my abilities.

This thesis is dedicated to Teddy, who is always there to put a smile on my face, and Bailey, whose loving memory stays with me every day. They continue to fuel my interest in research aimed at improving treatments for patients living with metabolic disorders.

Table of Contents

List of Figures

List of Tables

Chapter 1: Introduction

1.1 Diabetes

Developments in healthcare and medicine emerge regularly. While new advances have been used to cure or manage various diseases, there is a growing concern about new health problems and in particular, noncommunicable diseases such as type 2 diabetes, cardiovascular disease, hypertension, and stroke[1]. Type 2 diabetes is of importance as it has become one of the top five leading causes of death in most countries[1]. This statistic may even be an underestimate since diabetes tends to be under-reported on death certificates[2]. In one study published in 2007, it was estimated that 4.6% of adults were affected by diabetes worldwide and by 2030 that value could increase to 6.4%[3].

It is apparent that diabetes is a significant health concern. Not only does diabetes have a large health impact on society, it also causes economic burdens. These economic costs take into account the treatments for diabetes itself and also related complications such as limb amputations, blindness, and kidney failure[4]. In Canada, the cost of diabetes in 2000 was estimated at $6.3 billion annually[5]. It was predicted that this number would increase substantially by 2020 to $16.9 billion annually[5]. It is clear that diabetes will be a growing economic drain on our economy. Diligent efforts are needed to find ways to prevent an increase in the number of patients with diabetes and more effectively treat those already afflicted with the disease.

Diabetes mellitus can be characterized by deficiencies of insulin in the body which cause disturbances in the metabolism of carbohydrates, proteins, and fats[6]. There is a decrease in the movement of glucose into adipose tissue and skeletal muscles, which also

leads to a decrease in glycogen formation[6]. This combination of events causes hyperglycemia in the patient. If the blood sugar becomes sufficiently high, glucosoria will occur where the kidneys will excrete the excess glucose from the blood into the urine[6]. This causes a greater excretion of water and electrolytes from the body due to an increase in osmotic pressure, leading to a state of polydispia where the patient becomes increasingly thirsty due to dehydration[6].

Two different classes of diabetes exist: Type 1 and Type 2. Type 1 affects 5-10% of diabetic patients[6]. Type 1 diabetes can be considered insulin dependent diabetes (IDDM) and is sometimes referred to as juvenile onset diabetes[6]. It develops when there is an autoimmune destruction of β cells which control insulin production[6 7]. Eventually, the β cells will cease to produce insulin altogether[6]. Insulin use is then mandatory therapy[6 7], however it is difficult to achieve blood glucose levels that are as stable as those of non-diabetics[6].

Type 2 diabetes is the more prevalent form of the disease, making up roughly 95% of the cases that occur in the United States[7]. This class of diabetes typically occurs in individuals over the age of 40 and is sometimes referred to as maturity-onset diabetes or non-insulin dependent diabetes (NIDDM)[6]. It is caused by a decrease in the body's sensitivity to insulin and also a decrease in insulin secretion[6 7]. The decreased sensitivity causes the body to behave as if it is not producing sufficient amounts of insulin to maintain normal metabolic processes[6]. This in turn leads to the β cells working harder in attempting to overcome the state of insulin resistance in the surrounding muscle and fat cells[6]. Type 2 diabetes can be controlled using insulin therapy, hypoglycemic drugs, or a combination[7]. Hypoglycemic drugs can function in a variety of ways, including

stimulating insulin production by the pancreas, decreasing hepatic glucose production, or increasing glucose uptake by muscles[8]. These drugs alone can be effective in managing the condition, but continual decline in β cell function will eventually require the use of insulin therapy to effectively treat the patient[7].

1.2 Insulin Therapy

1.2.1 Subcutaneous Injection

Insulin therapy is currently administered through subcutaneous injection. While this method has been used for a number of years, there are some inherent problems that necessitate a more effective delivery system for insulin. One major problem is that insulin injections expose all of the body's tissues to an equal concentration of insulin, providing the liver with only a fraction (~20%) of what was initially injected[9 10]. This overexposure in many tissues can cause negative effects, including overstimulation of cell growth and other metabolic events that can lead to diabetic complications[9 10]. In contrast, physiological insulin is produced in the pancreas and secreted into blood vessels[10]. Insulin then enters hepatic portal circulation where it contacts the liver, which acts as a regulator[11]. The insulin may then be destroyed by the liver before entering general circulation[11]. It is obvious from this mechanistic difference in insulin delivery that it is not possible to mimic the normal pattern of basal insulin secretion, causing patients to experience hyperinsulinemic episodes[8]. Therefore, it would be beneficial to develop a method of insulin delivery that more closely mimics the body's natural insulin pharmacokinetic profile[6 7].

There are also issues related to the negative effects the delivery method itself can have on a patient's life. These can include inconvenience, trauma, pain, anxiety, and social stigmas[12], leading to poor patient compliance. Improper treatment of diabetes can have serious consequences to the patient and even be life threatening in some cases. These are important reasons why an improved delivery method for insulin is necessary to improve patient compliance and overall quality of life.

Many different techniques for overcoming these ongoing problems have been developed and tested. Several companies have become involved in this area of research with a number of ideas being evaluated in clinical trials. Different delivery routes have been applied, including buccal, pulmonary, and oral. **Table 1** summarizes select examples of different approaches to insulin delivery.

Table 1. Examples of companies researching alternative delivery routes for insulin

Company Name	*Technology Description*
Emisphere Technology	Eligen® Technology: developing oral dosage forms for poorly absorbed compounds (Phase II Trials)[13]
Generex Biotechnology	Generex Oral-lyn™: buccal insulin delivery absorbed through inner mouth lining (Phase III Trials)[14]
Pfizer/Nektar Therapeutics	Exubera: inhalable insulin (no longer manufactured)[15]
Oramed Pharmaceutical Inc.	Oral insulin capsule (Phase II Trials)[16]
Novo Nordisk	Oral insulin analogue (Phase I Trials)[17]
Diabetology	Capsulin™ OAD oral insulin (Phase II Trials)[18]

Chapter 2: Literature Review

2.1 Oral Delivery

One alternative route of insulin delivery that is of significant interest is oral delivery. There are many advantages to considering an oral delivery route for insulin that would potentially help to rectify the problems described. The oral route would more closely mimic the effects of natural insulin, helping to improve glucose homeostasis and avoid peripheral hyperinsulinemic effects caused by insulin injections[19]. This would greatly improve the treatment of diabetes and decrease the occurrence of complications. Other advantages are related to patient comfort and lifestyle. Oral insulin delivery would be a noninvasive, convenient, and easily dosed method of drug delivery[9]. Also, oral doses would eliminate complications due to the need for sterile technique when using injectable insulin[9]. All of these benefits would improve patient compliance which is critical in treating a chronic condition like diabetes[7 9.]

Oral insulin delivery presents many advantages over insulin administration via subcutaneous injection but there are also many challenges to overcome in developing a successful drug delivery technology. The first challenge is that insulin, as well as all other proteins and peptides, is susceptible to proteolytic and hydrolytic degradation throughout the gastrointestinal tract (GIT)[9]. Proteolysis begins in the stomach where pepsin will begin to break down the insulin[9]. Overall, 10-20% of total protein degradation is accomplished by pepsin[9]. The stomach is also an acidic environment which is potentially damaging to insulin's three-dimensional structure[6]. Once in the

small intestine, insulin is still susceptible to degradation by the action of trypsin, chymotrypsin, and carboxypeptidases[20].

In addition to being susceptible to degradation, insulin, like other proteins, is poorly absorbed across the intestinal barrier. The mucus gel layer and epithelial cells both lead to poor intrinsic permeability through the intestinal membrane[21]. There is rapid clearance of proteins from the site of absorption[22], and absorption can also be limited by the metabolic activity of the microflora in the lower small intestine and the large intestine[21]. Additionally, insulin has inherent characteristics that limit its absorption, including its large molecular size relative to metabolites, electrical charge, and hydrophilicity[21]. The combination of these properties severely limits the amount of insulin that will absorb across the intestinal membrane. Also, if the tertiary structure of the insulin is altered at any point in the GIT, the biological activity will change potentially leading to inactivation of the protein[20].

There is a need to develop a drug delivery system for oral insulin that will aid in overcoming the many barriers inherent to the GIT. The main criteria for any possible delivery system are that it provides sufficient protection from the harsh environment of the stomach, enhances absorption across the intestine, and maintains the biological activity of the insulin. A summary of the specific objectives in the design of an oral insulin delivery vehicle are summarized in **Table 2**.

Table 2. Requirements for oral insulin delivery device

Provide insulin with stable and biocompatible environment[23]
Preserve physiological activity during formulation and delivery[23 24]
Protect from enzymatic degradation[22 24]
Enhance absorption through intestinal mucosa[22 25]
Small carrier size to facilitate uptake[24]
Balance between hydrophobic and hydrophilic surface properties[24]

2.2 Polymer Systems for Insulin Encapsulation

Polymeric encapsulation of insulin is an interesting approach to insulin delivery. Encapsulation is thought to protect insulin from enzymatic degradation and from the changing environment of the GIT, potentially preserving the biological activity of the drug. Encapsulation can also aid in the transport of the insulin across the intestinal membrane. The choice of polymer that will best address the goals listed in Table 2 accounts for a large area of ongoing research.

The use of natural polymers, especially polysaccharides, is an option currently being considered. Examples of compounds used for this application include alginate, chitosan, and dextran. The advantages of natural materials include biocompatibility, biodegradability, natural abundance, and unique chemical structures[25 26 27]. The obstacle to polymers of natural sources is that their structure is fixed, limiting the flexibility to modify the properties[28].

2.2.1 Alginate

A frequent choice of polymer for insulin encapsulation is the polysaccharide, alginate (poly [1-4)-β-D-mannopyranosyluronate-(1-4)-α-L-gulopyranosyluronate (1-4]). Alginates are isolated from brown algae such as *Laminaria hyperborea* and *Laminaria lessonia*[25] with a dilute alkaline solution, solubilizing the alginic acid, which is often converted to a salt, most commonly sodium alginate[29]. Alginates are a class of linear unbranched polymers consisting of 1,4'-linked β-D-mannuronic acid (M) and α-L-guluronic acid (G) residues[6 25]. These components are arranged in blocks, which can be either similar (MMMMM, GGGGG) or alternating (GMGMGM)[6 25 29]. An example of a polymer chain of alginate is seen in **Figure 1.**

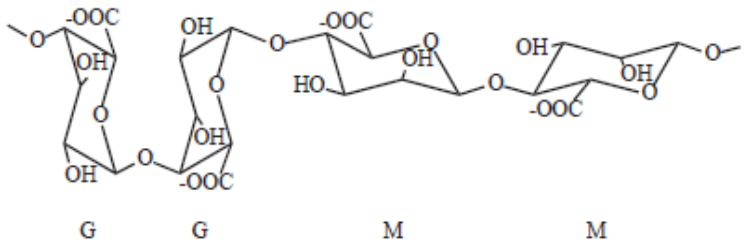

Figure 1. Alginate polymer chain with two M and two G residues connected by (1,4)-linkages[30]

The two isomers (M and G) have slightly different properties, allowing the characteristics of alginate to vary as the composition of the polymer varies. As a rule, G blocks are noticeably stiffer than alternating blocks[25], therefore alginates with a high G content have significantly greater strength compared to those that have a higher M content[29]. The M/G ratio is important because a polymer with greater amounts of G will produce a higher degree of coordination to the cation[29] forming a rigid gel that is more

resistant to swelling and erosion[29]. If the alginate has a higher M content, the gel will be softer and more elastic, making the gel less porous and more readily dissolvable[29].

Alginate delivery systems are often based on diffusion where insulin is released from the alginate system by diffusing through the pores of the bead or particle. One encapsulation technique is the polymer membrane system in which the drug is encapsulated within an open compartment in the bead[29]. This strategy is based on the specific permeability of the membrane and can be done using microencapsulation or spray drying[29]. The other diffusion-based technique is the polymer matrix system. In this system, the drug is homogenously combined with the polymer matrix[29]. The drug can be incorporated into the polymer in one of two ways: drug loading after the alginate has been crosslinked to form a bead or incorporation into alginate solution prior to cross-linking[6]. After loading, the drug can be released from the bead or particle by diffusion through the pores of the alginate network or by the degradation of the network[6].

The alginate solution must be immobilized to form beads to successfully encapsulate the insulin. Some immobilization methods involve the use of organic solvents, high temperatures or extremes in pH, conditions that could potentially interfere with the biological activity of the drug being encapsulated[31]. A gentler method was developed where an ionic polysaccharide solution, such as alginate, would be extruded dropwise through a syringe needle into a divalent cation solution (usually Ca^{2+} for alginate systems)[31]. The charged species on the polysaccharide is cross-linked with the divalent cation in the solution[32]. Cross-linking forms insoluble, spherical gel beads[32]. A related immobilization technique is emulsification/internal gelation. This technique involves the gelation of an alginate solution within an oil dispersion[31]. Internal gelation is achieved

through the release of calcium ions from an insoluble complex such as calcium carbonate. This is done by a small pH adjustment through the addition of an oil soluble acid which will partition into the aqueous alginate phase[31]. This method allows for the generation of beads with smaller diameters, usually within the range of 200 – 1000 μm[31], however there is a large dispersion in the bead diameters.

2.2.2 Chitosan

Coatings are often applied to alginate beads to help improve the retention of encapsulants including insulin. One polymer that is used frequently is chitosan (poly-(1-4)-2-amino-2-deoxy-ß-D-glucan), which forms a stable and tight complex with alginate, and helps prevent leakage of insulin. Chitosan also improves the mucoadhesive properties of the delivery device and encourages uptake by reversibly opening tight junctions between epithelial cells[33 34]. Chitosan is derived from chitin, which is found in a number of sources including crustacean shells, cell walls of fungi, and insect exoskeletons[35]. The chitin is partially deacetylated to form chitosan which is a polysaccharide that is a copolymer of glucosamine and N-acetylglucosamine[36]. This polymer is insoluble in solutions of neutral or alkaline pH but will form salts with organic and inorganic acids including glutamic, hydrochloric, lactic, and acetic acid[36]. When chitosan dissolves in acid, the amine groups are protonated, resulting in a positively charged soluble polysaccharide[36]. Some common chitosan salts are chitosan glutamate and chitosan chloride. **Figure 2** was adapted to show structures of chitin, chitosan as a polyamine, and chitosan in its cationic form[37].

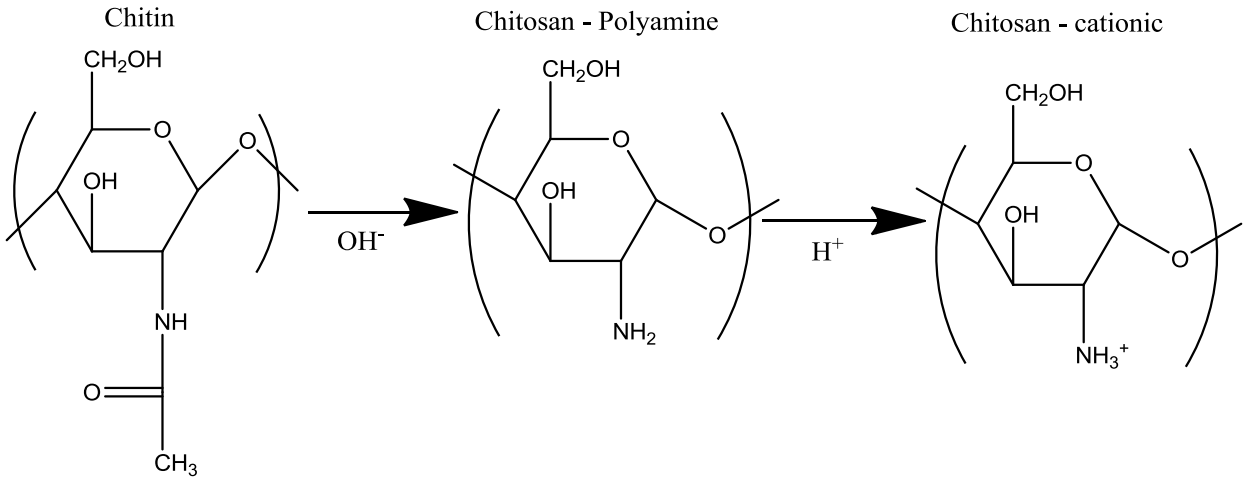

Figure 2. Structures and forms chitin and chitosan, modified from reference [36]

Chitosan salts are readily soluble in water, and the solubility depends on the degree of deacetylation and the pH. Higher degrees of deacetylation result in a polymer that is less soluble in higher pH solutions[36]. Solubility of chitosan salts is also dependent on salt additions to the aqueous solution. Solutions with a higher ionic strength will decrease the solubility of the chitosan salts[36]. Increasing degree of deacetylation also increases the viscosity of the chitosan solution due to conformational changes that occur in the chitosan itself. If there is a high degree of deacetylation, the chitosan is highly charged, resulting in an extended conformation with more flexible chains[37]. Lower degrees of deacetylation result in chitosan that has a more rod-like or coiled shape due to a lower polymer charge[37].

Due to its pH responsive properties, chitosan has the potential to be useful in controlled release situations, allowing a prolonged therapeutic effect[36]. In addition, chitosan has mucoadhesive properties which can promote retention and absorption of the

drug in the intestines[27] [36]. It does so by adhering to mucus tissues lining the GI tract, and reversibly opening the tight junctions between epithelial cells[24].

In regards to oral insulin delivery, chitosan is used as a coating for insulin loaded alginate beads. Chitosan does not change the overall size or shape of the beads, but will alter the surface and the internal structure[38]. In one study where bovine serum albumin (BSA) was used as a model protein for encapsulation, a noticeable increase in drug retention was seen for alginate beads with chitosan[38]. Uncoated alginate beads retained 43% of originally loaded BSA, while the chitosan coated beads were able to retain 70% [38]. This reduction in the release rate of BSA was thought to be due to the chitosan membrane coating, formed through an ionic interaction with the alginate core[38]. This membrane coating improves encapsulation by preventing release of BSA through the less porous chitosan membrane. The optimal concentration for the chitosan coating solution was 0.3% in 0.01 M HCl. BSA is a poor model for insulin since BSA is a much larger protein. The results obtained may have been different if insulin had been used instead of BSA.

2.2.3 Dextran

Dextran is another polysaccharide polymer that is used in combination with alginate and other polymers for the encapsulation of oral insulin. It is a branched polysaccharide made up of α-D-glucopyranosyl residue components[39]. Dextran is predominantly composed of α(1→6) linkages, however other linkages such as (1→2), (1→3), and

(1→4) can be incorporated into the structure[39]. The structure of dextran is illustrated in **Figure 3**.

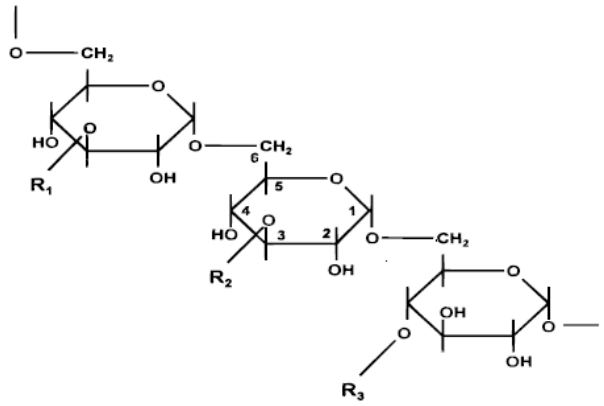

Figure 3. Structure of dextran[39]

Dextran can have varying degrees of branching, but the type used most often commercially is made from *Leuconostoc mesenteroides* and has a degree of branching around 5%[40]. The exact branched topology of dextran is not as well known as it is with other branched polymers like amylopectin and glycogen.

A common use for dextran is in blending with other polymers to improve the overall properties of the drug delivery device. Dextran is blended with alginate to slow overall drug release[41]. It is commonly used in the form of dextran sulfate which has negatively charged sulfate groups[41]. This polyanion is biodegradable and biocompatible and has been frequently used as a matrix material to control drug release or as a stabilizing agent[41 42 43].

An insulin loaded alginate-dextran nanopolymeric delivery system was examined in an *in vitro* release study simulating gastrointestinal conditions[23]. At the low pH gastric condition, the insulin was fully retained in the particles, explained by the alginate

polymer forming a more compact acid-gel structure, reducing the permeability of the particle and further protecting the insulin from the harsh acidic conditions[23]. The particles were then subjected to more neutral conditions representative of the intestine. It was found that 89% of the insulin was released right away with complete release after one hour thought to be caused by both the alginate and the insulin being negatively charged at neutral pH leading to electrostatic repulsion, promoting insulin release[23].

It appears that alginate and dextran in combination are not effective in preventing the release of insulin at neutral pH. Therefore, other components need to be incorporated to develop a successful oral delivery device for insulin, such as adding a coating material like chitosan. This was the approach taken in one study where the insulin was encapsulated in a core made of alginate, dextran, and poloxamer. These cores were subsequently coated with chitosan and bovine serum albumin (BSA).[44] The alginate/dextran cores were formed through ionotropic pregelation followed by polyelectrolyte complex coating, with poloxamer added to avoid nanoparticle aggregation and reduce enzyme adsorption[45]. The chitosan and BSA coatings were applied via polyelectrolyte complexation. The role of the BSA was to act as a sacrificial coating to protect the core from proteolytic degradation. The results of an *in vitro* release study showed that almost all of the insulin was retained in the particles under gastric conditions, however most of the insulin is released after one hour once exposed to intestinal conditions. *In vivo* results indicated that the insulin-loaded nanoparticles had an improved pharmacological effect compared to free insulin, which was also administered orally. Also, the nanoparticles lowered blood glucose levels at a faster rate

than free insulin, indicating a better internalization of the insulin following oral administration.

2.3 Evaluation of Oral Insulin Delivery Systems

There are a large number of different delivery systems being studied to facilitate oral insulin delivery. Due to the unproven application of these different delivery devices, it is important to have reliable methods of evaluation to assess the effectiveness. Insulin retention and release from the delivery device is commonly evaluated *in vitro* before being subjected to *in vivo* tests. The method of *in vitro* testing is crucial when evaluating a new drug delivery system for oral insulin because the *in vitro* tests must provide an accurate assessment of the behavior of insulin or the delivery vehicle when administered *in vivo*.

There are cases where the *in vitro* and *in vivo* results contradict, indicating that the *in vitro* testing method may not be a reliable predictor of how the drug delivery device behaves in the body. In many studies, the *in vitro* release results indicate that the majority of the insulin is released from the delivery device rapidly upon entering the small intestine. *In vivo* testing, on the other hand, reveals that a significant amount of the insulin is pharmacologically available within the body[44 46]. In one study using nanoparticles, the pharmacological availability of the encapsulated insulin was 11% but 100% release was measured after 1 h in intestinal fluid during an *in vitro* study[44]. It has been suggested that bioavailability values between 10 and 20% are significant for clinical application[47]. Subcutaneous insulin injections may not be completely replaced but oral doses could reasonably supplement overall treatment. In another study involving

nanospheres, nearly 75% of insulin was released after 2 hours in intestinal fluid during an *in vitro* study, but the pharmacological availability was determined to be 42%[46]. High availability can indicate that the delivery system was able to deliver insulin at a place along the GIT that promotes greater uptake. This can be accomplished by insulin release at absorption sites in the intestinal mucosa or the direct uptake of the delivery system itself. Such high insulin *in vitro* release should indicate that little should be pharmacologically available. From these conflicting results, it is assumed that the *in vitro* testing method does not accurately mimic conditions seen *in vivo*. It is then necessary to improve the predictability of the *in vitro* model since it is a simple and inexpensive method of evaluating the behavior of various drug delivery devices.

Many different *in vitro* models of the gastrointestinal tract (GIT) are being studied and evaluated. The different models range in design and complexity and are often tailored to best evaluate the specific delivery device being tested. These models are based on the known mechanics of the GIT and the properties of digestive fluids.

2.4 Stages of Digestion

2.4.1 Mastication

Digestion first begins in the mouth with mastication. The food at this point is broken down mechanically with chewing and chemically with saliva. Chewing reduces the size of the food particles, increasing the available surface area. The smaller particles are exposed to amylase and lipase in the saliva which begins the chemical breakdown component of digestion. Chemical and physical breakdown aids in the formation of a bolus which is then transferred down the esophagus into the stomach for the next phase

of digestion. The size of particles at the end of mastication is highly dependent on the texture of the food ingested. It has been shown that the rate of breakdown is inversely dependent on a characteristic referred to as the fragmentation index, based on the food's toughness and the Young's modulus indicating material strength.[50]

2.4.2 Stomach

Digestion continues in the stomach where the main goal is to transform the food into chyme. This entails altering both the physical and chemical characteristics of the food material, including particle size, pH, osmolarity, caloric density, and liquid viscosity[48]. The overall shape of the stomach resembles that of a vertical 'J', though its specific shape can fluctuate depending on the contents and influence of other organs[48]. The stomach is referred to by distinct segments which can be seen in **Figure 4**.

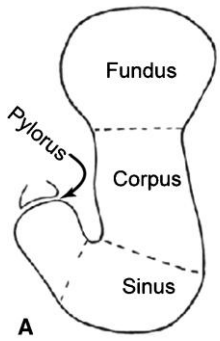

Figure 4. Segments of the stomach[48]

The vertical section of the stomach has two segments, the fundus and the corpus. The fundus is hemispherical in shape and the corpus is shaped as a cylinder. These vertical sections act as a reservoir for foods that have been consumed recently[49]. The other segments are part of the horizontal stomach, including the pylorus, where the food is

emptied from the stomach. Since the stomach acts in part as a reservoir, it has the ability to expand to accommodate varying amounts of material. The stomach is able to stretch to a maximum volume of around 4 liters[50].

As food is consumed, it is layered within the stomach. As each layer moves progressively closer to the pylorus, it becomes a paste and then a liquid. Foods are layered according to order of consumption and material density. This behavior is represented in **Figure 5**, showing the general pattern of food layering that occurs.

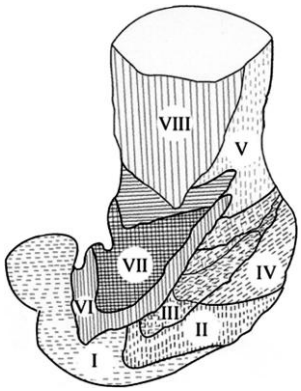

Figure 5. Layering pattern in the human stomach[48]

As seen, layers near the top of the stomach are stacked vertically, whereas those that have spent more time in the stomach have spread out forming more horizontal layers. All of these layers are gradually exposed to gastric secretions throughout the entire stomach pathway.

The contents of the stomach are agitated via peristaltic contractions, which generally occur at a rate of 3 cycles/min in humans and propagate at a speed of 2.5 mm/s[51]. The type and quantity of a meal can have a large effect on the specific behavior of the contractions in terms of amplitude, propagation length, and duration of peristalsis.

Contractions can last for minutes as when digesting liquid meals, or several hours for large solid meals, since digestion rate is affected in part by how long it takes the enzymes to break down the material present[53]. The two largest components present in gastric juice are pepsin and mucin. Pepsin is present at a concentration of 0.8 – 1 mg/mL and mucin accounts for a slightly larger proportion at 1.5 mg/mL[50]. Once the contents of the stomach reach the pylorus, one of two things can occur. First, some of the material is able to leave the stomach through the relaxed pylorus. Otherwise, the material is returned to the stomach for more digestion and agitation. The size requirement for particles to leave the stomach is 1 – 2 mm[52]. This dynamic process is represented schematically in **Figure 6**.

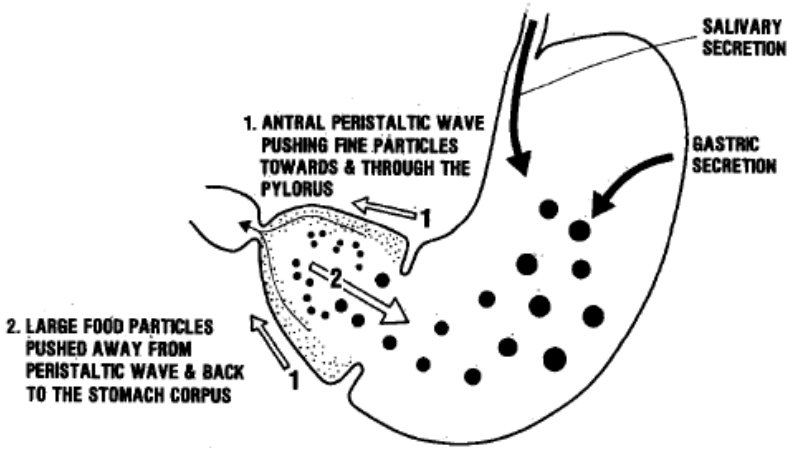

Figure 6. Pattern of gastric digestion[53]

In general, different meal types will pass through the stomach at varying rates. Liquid meals generally experience first order kinetics, where the emptying rate is dependent on the liquid volume, whereas solid meals exhibit zero order kinetics with no dependence on volume.[48]

2.4.3 Intestines

Once chyme leaves the stomach, digestion enters the next phase within the duodenum of the small intestine. Chyme is exposed to more physical and chemical breakdown to reduce particle size to a point where nutrient molecules are able to pass across the intestinal barrier. As in the stomach, the material is exposed to contractions that promote mixing and particle breakdown to ensure exposure to pancreaticobiliary secretions, which include trypsin, chymotrypsin, and carboxypeptidases[48]. The segmental contractions cause a back and forth motion of the food material and act as a mixing mechanism.

2.5 *In vitro* modeling of the GIT

Digestion is a complicated process making *in vitro* modeling difficult. Different models have been developed to describe the sections of the GIT with varying degrees of complexity and accuracy in terms of physiological representation. Models tend to be adapted to the specific situation and often focus on just one of the sections of the GIT: mouth, stomach, small intestine, or colon. Mastication models are often studied to look at chewing time and particle size after chewing, since different foods are broken down at different rates in the mouth. One study compared the characteristics of chewing for two different foods, bread and pasta[54]. Chewing times varied significantly, with bread at 27 seconds and cooked pasta at 20 seconds. The two different materials showed differences in final size and shape at the point of swallowing. Bread was transformed into small particles between 5 and 1500 μm. The cooked pasta was reduced to small cylinders with lengths of 2.5 – 30 mm. Differences in the final chewed pieces can be seen in **Figure 7**.

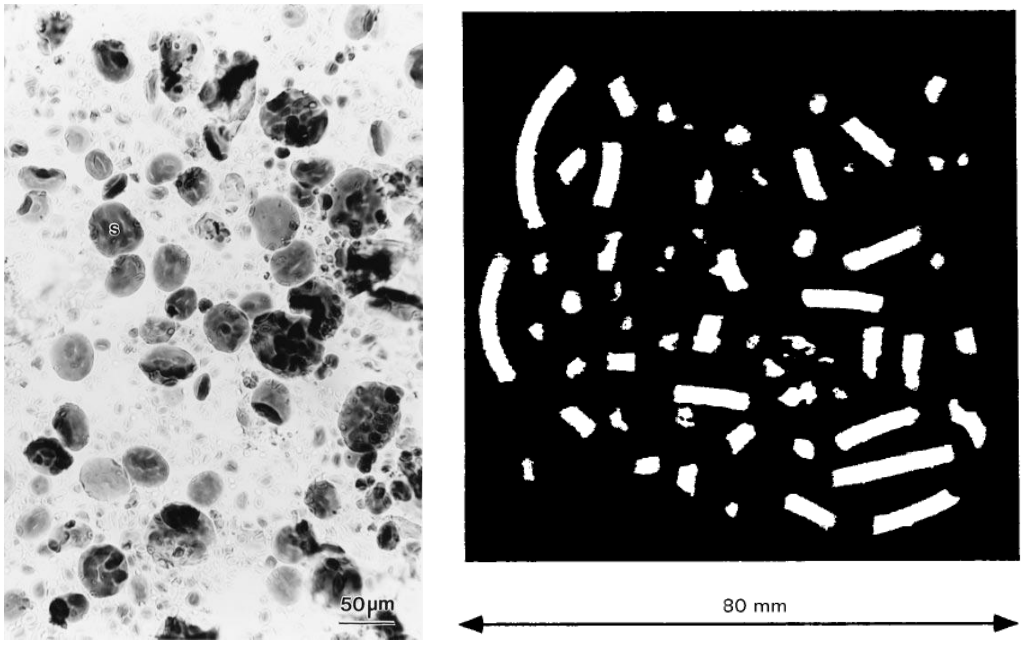

(a) **(b)**

Figure 7. Particles of chewed bread (a) and chewed spaghetti (b)[54]

From these images, it can be seen that the type of material being ingested has a major impact on the mechanism and overall result of chewing. These differences must be kept in mind when designing an accurate *in vitro* model of mastication.

One simple model of mastication involves the technique of manual mincing using a meat mincer[55]. This *in vitro* chewing method proved to be reasonably accurate for mimicking the effects of mastication with reasonable distributions in particle size. The size distribution for bread was higher than the distribution for pasta but both fell within a satisfactory range. Overall, this simple *in vitro* model of mastication is an easy to use option for routine testing of the effects and patterns of mastication.

The stomach is a very commonly modeled component of the GIT, focusing on both its unique motions and many chemical components. One model example focuses largely on

the peristaltic motions of the stomach and the resulting flows of different types of particles[53]. A schematic image of the model can be found in **Figure 8**.

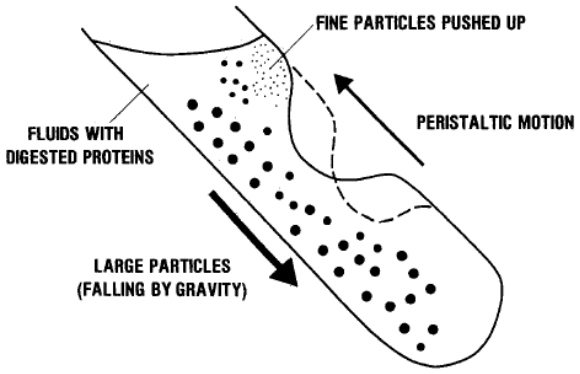

Figure 8. *In vitro* model of peristaltic motion and particle flow in stomach[53]

This model consists simply of a tygon tube with a peristaltic pump. The angle for the device was designed to encourage the particle motion depicted in the figure. This device was developed to look at the major components of digestion within the stomach including the method of agitation, composition of gastric fluid, and residence time.

Models of different GIT components are often applied sequentially in studies. One example focused on combining the effects of both mastication and gastric digestion[56]. This model applied a previously developed chewing method[55] with the addition of chemical components to mimic salivary digestion. Saliva composition was modeled with phosphate buffer and pancreatic amylase. The gastric digestion component was modeled very simply with an Erlenmeyer flask agitated with an overhead paddle stirrer. The pH and enzymatic composition were controlled by addition of HCl and pepsin solutions. The gastric vessel and regulating components are depicted in **Figure 9**.

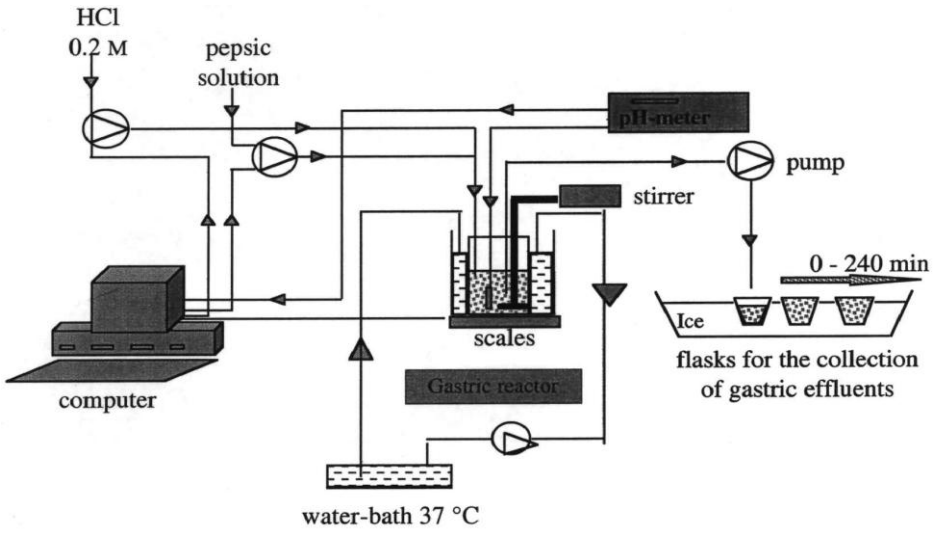

Figure 9. Model of a gastric vessel and its related controls[56]

This particular model of mastication was the first time that the concept of chewing had been combined with enzyme effects. The sequence of physical breakdown of food, then exposing it to pancreatic amylase was deemed an acceptable approach with limited complications. The gastric model also proved successful in mimicking the overall effects of the stomach in terms of enzyme and pH conditions, as well as the workings of gastric emptying.

Other models of the GIT have examined the effects of the small intestine, as well as the mouth and stomach. One model focused more on the composition of the different digestive fluids while keeping the method of agitation consistent with simple rotating motion[57]. The samples are exposed to saliva, gastric juice, duodenal juice and bile before analysis of the final product. The sequential steps of the *in vitro* procedure are represented in **Figure 10**.

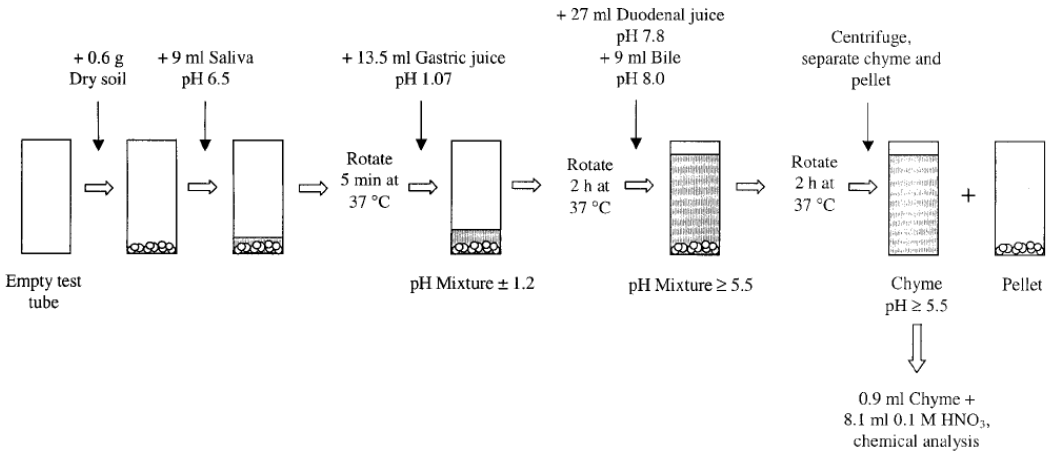

Figure 10. ***In vitro*** **digestion procedure modeling mouth, stomach, and small intestine**[57]

This model was designed specifically to look at the effects of soil ingestion as a significant cause of human exposure to soil contaminants. The model was able to mimic many different physiological components of the GIT while still remaining relatively simple to use for routine testing of a large number of samples. A second study used this same model to evaluate the effects of food contaminants[58]. Slight variations were applied to evaluate the implications on the bioaccessibility of different contaminants. Again, the model was seen to be extremely useful for routine testing, however further work needs to be completed to validate the model against *in vivo* conditions in humans.

The models discussed until now have been focused on the conditions of the upper GIT, eliminating components of the colon. Still, models do exist that focus directly on the behavior and effects of this last component to digestion. One such model is referred to as the Simulated Human Intestinal Microbial Ecosystem (SHIME) reactor[59], which models both the small intestine and colon. This model is a five-stage system with each compartment agitated by magnetic stirring. Each vessel also has appropriate ports for

testing, sampling, and adding or removing components. A diagram of the overall system is displayed in **Figure 11**.

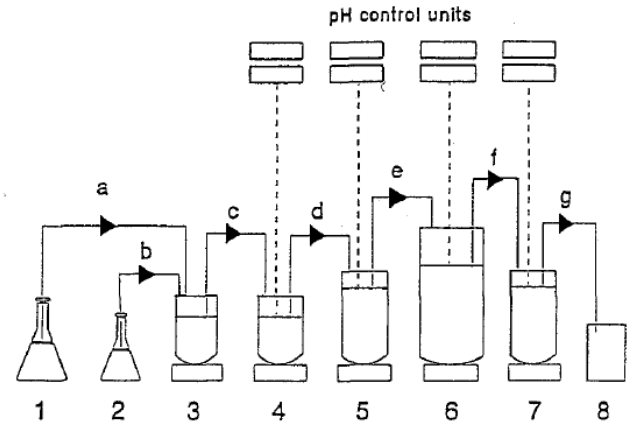

Figure 11. Simulated human intestinal microbial ecosystem (SHIME) reactor: (1) feed (2) pancreatic acetone powder (3) stomach (4) small intestine (5) colon ascendans (6) colon transversum (7) colon descendans (8) effluent[59]

An evaluation of the system revealed that the model was valid for testing principal interactions of the different microbial components. As with any model, comparisons against *in vivo* results are important to validate the system. Any differences found need to be accounted for when analyzing results and improvements should be made to limit discrepancies in data. One of the discrepancies found between the model and *in vivo* conditions was a higher than expected concentration of bacteria in the first compartment. More complex conditions *in vivo* would likely account for lower amounts of bacteria present. Another difference between the model and actual conditions in the human body is that hydrogen was expected to be present in the fifth compartment but was only detected in the third compartment for certain conditions.

This model was used in a subsequent study looking into the effects and potential improvements of soygerm powder on the intestinal microbial environment[60]. Soy food products have been extensively studied for the implications in lowering incidences of cancers, cardiovascular disease, and osteoporosis. The SHIME *in vitro* model was deemed a successful tool at evaluating the questions of interest in this study and is a good representation of the effects of soy on the conditions of the intestine.

Most *in vitro* models have been developed in academic labs for specific research studies. However, a commercially available device has been developed by TNO in the Netherlands. TNO developed two systems to model the upper GIT and the large intestine, referred to as TIM-1 and TIM 2 respectively[62] [61]. Both systems are able to control all major functions and reactions that occur within the GIT, including pH changes, peristaltic movements, temperature, incorporation of enzymes, and absorption of digested materials. The TIM-1 modeling the stomach and small intestine is shown in **Figure 12**.

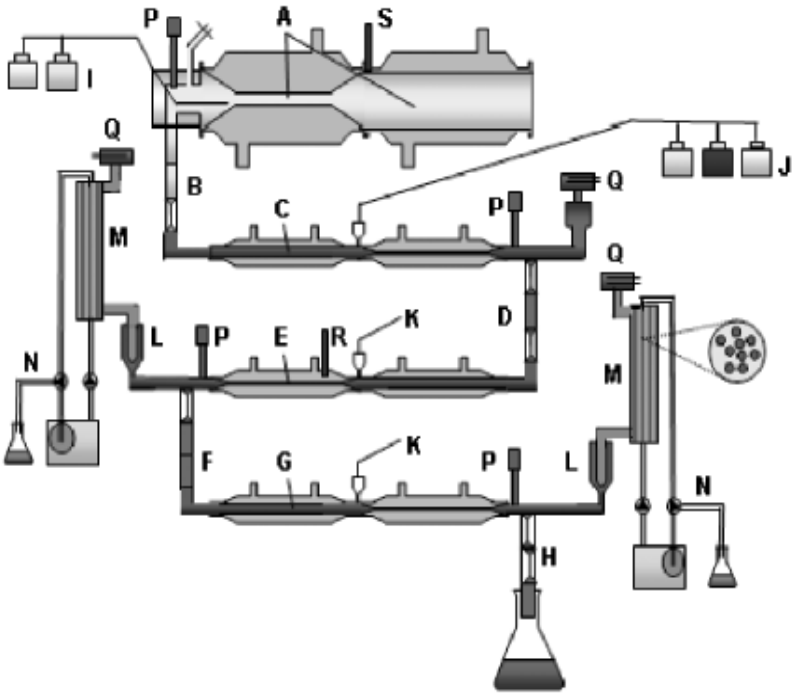

Figure 12. TIM-1 schematic diagram[62]

Each of the different compartments represents a section of the upper GIT: (A) stomach, (C) duodenum, (E) jejunum, (G) ileum. Each compartment is made of a flexible material within a water-filled glass jacket that controls temperature and pressure and helps simulate the compression relaxation cycle seen throughout the GIT.

The TIM-2 system models the complexities of the large intestine. **Figure 13** is a diagram of the equipment followed by **Table 3** labeling all individual components.

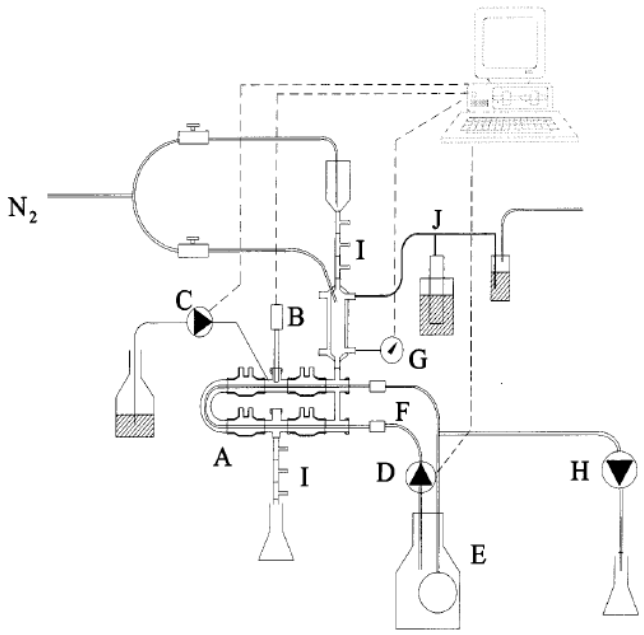

Figure 13. TIM-2 schematic diagram[61]

Table 3. TIM-2 components[61]

Diagram Label	Component
A	Mixing unit
B	pH electrode
C	Alkali pump
D	Dialysis pump
E	Dialysis light
F	Dialysis circuit
G	Level sensor
H	Water absorption pump
I	Peristaltic valve pump
J	Gas outlet

As with the TIM-1 system, the walls of the vessels are manipulated to form peristaltic waves to agitate and move the contained material. The TIM-1 and TIM-2 systems are designed to work together, and controllers are used to monitor and control various parameters. The systems have been used to evaluate both digestion of foods and uptake of drugs indicating that it is applicable for testing in many different scenarios.

The development of a drug delivery device for the application of oral insulin is a continuing challenge for many researchers. Many different techniques have been attempted including insulin encapsulation within natural polymers, including alginate, dextran, and chitosan. Different elements are used together or applied as coatings to best protect the insulin and promote absorption across the small intestinal barrier.

With optimization, oral insulin delivery with the use of natural polysaccharides is a feasible alternative to current insulin therapy methods. Not only would it improve patient compliance and quality of life, it would also deliver insulin to the body in a way that is more comparable to physiological insulin. There are a significant number of patients with diabetes worldwide, making this area of research a worthwhile endeavor that has the potential to have an impact on available therapies for diabetes.

These many potential drug delivery devices are commonly evaluated with *in vitro* testing methods before animal testing is employed. Many different *in vitro* models have been designed for testing in a wide variety of situations. Different models focus on different components of the GIT, including mechanical agitation, fluid components, digestion time, and emptying techniques. These models vary greatly in terms of complexity and accuracy with respect to how well the model predicts the behavior of the delivery device *in vivo*. While many advancements in physiological modeling have been accomplished including the development of a complex commercial model, many improvements can still be made to facilitate routine testing of the behavior of various oral insulin delivery devices.

There are many barriers to oral insulin delivery that can be considered when developing a model of the GIT to be used for *in vitro* testing. Some of the barriers are listed in **Table 4.**

Table 4. GIT barriers to oral insulin delivery

Proteases present in saliva, stomach, and intestines
Acid hydrolysis in gastric fluid
Clearance from intestines by mucus layer before insulin can effectively contact the epithelial cells
Difficulties for insulin passing across epithelial barrier in intestines
Premature insulin release from delivery device
Lysozyme degradation of chitosan
Microorganisms degrading insulin or delivery device components such as dextran
Large molecular size of insulin and other intrinsic properties

In this study, the barriers that will be addressed during modeling include proteases in the stomach and small intestine and acid hydrolysis in gastric fluid while trying to mimic the motions that occur along the GIT. These factors affect the amount of insulin in the oral delivery device that will be pharmacologically available in the body. Insulin can be prematurely released from the delivery system or can be degraded or structurally altered by acid hydrolysis or gastrointestinal enzyme degradation. It is imperative that these issues be addressed in order for an oral insulin delivery technique to be successful.

Chapter 3: Objectives

Diabetes treatment is a highly advanced field of research, but there remains considerable interest around methods to improve insulin delivery. Oral insulin delivery has many advantages over subcutaneous injection, including physiological benefits and improved patient comfort and compliance. Natural polymers are common materials used to develop oral delivery devices through encapsulation. Alginate, dextran, and chitosan are some of the most widely used natural polymers for this application. Different devices are commonly evaluated *in vitro* before being tested *in vivo*. Previous studies have shown that there is a difficulty with *in vitro* testing methods since they are often not accurate predictors of what will happen during *in vivo* testing.

A need exists for a simple *in vitro* model of the GIT that will more accurately mimic the conditions within the body. It is thought that a more representative model will ensure that *in vitro* results are more reliable and will better predict the results of *in vivo* testing. The specific objectives in developing a simple model of the GIT for *in vitro* evaluations are listed as follows:

1. Design a simple, easy to use physiological model of the GIT focusing on conditions of the stomach and small intestine.
2. Evaluate different mixing methods to determine the best approach for *in vitro* agitation of selected oral insulin delivery devices based on analysis of mixing characteristics and results of release profiles in simulated gastrointestinal fluids.

3. Determine the effects of acid and protease hydrolysis on encapsulated insulin or prematurely released insulin in different GIT models using a simulated gastric fluid with pepsin.
4. Determine the effects of intestinal protease hydrolysis on encapsulated insulin or prematurely released insulin in different GIT models using a simulated intestinal fluid with trypsin.

Chapter 3: Materials and Methods

3.1 Materials

Tedlar® bags (500 mL) made of polyvinyl fluoride with a syringe port for sampling were purchased from Concept Control, Inc. (Calgary, Alberta, Canada). Novolin® ge Toronto human recombinant insulin (100 U/mL) manufactured by Novo Nordisk (Mississauga, Ontario, Canada) was purchased from a local pharmacy. Alginic acid sodium salt from brown algae (M_w 81,216, 250 cps) low molecular weight chitosan (50 kDa, 75-85% deacetylated), bovine serum albumin, dextran sulfate sodium salt from *Leuconostoc ssp.*, poloxamer 188 (Lutrol® F68), trypsin from bovine pancreas (10,000 BAEE units/mg protein), pepsin from porcine gastric mucosa, trypsin inhibitor from Glycine max (soybean), pepstatin A, and Fluorescein 5(6)-isothiocyanate were purchased from Sigma-Aldrich Canada Ltd. (Oakville, Ontario, Canada). Human insulin ELISA kits were purchased from Mercodia (Winston Salem, NC, USA). Micro BCA Protein Assay kits were purchased from Thermo Fisher Scientific (Ottawa, Ontario, Canada). Standard regenerated cellulose dialysis tubing (MWCO 3,500 Da) was purchased from Spectrum Labs (Rancho Dominguez, CA, USA). All other chemicals were of analytical grade.

3.2 Insulin Quantification

3.2.1 Micro BCA

Insulin in the microbead model was quantified with a Micro Bicinchoninic Acid (BCA) Assay. Insulin, as with other proteins, will reduce Cu^{2+} to Cu^{1+} which reacts with bicinchoninic acid to form a purple hued complex which is measured spectrophotometrically [63]. The protocol is applied to samples in a 96-well plate. 150 μL of sample is added to each well followed by the addition of 150 μL of working reagent. After a 2 h incubation on a plate shaker at 37°C, the plate is cooled to room temperature and the absorbance measured at 562 nm. The measurable range for insulin is 2 – 40 μg/mL. All samples were diluted within this range as was appropriate.

3.2.2 Human Insulin ELISA

Insulin in the nanoparticle and adjusted microbead systems was detected with a human insulin ELISA. This is a sandwich ELISA simultaneous assay, since the insulin binds to the antibody in the plate well and the detection antibody at the same time. After binding, any unbound components are washed away. An enzyme substrate solution is added that is converted to a chromogenic signal by the enzyme. Finally, this reaction is stopped by the addition of acid and the chromogenic product measured at 450 nm. This overall scheme is represented in **Figure 14**.

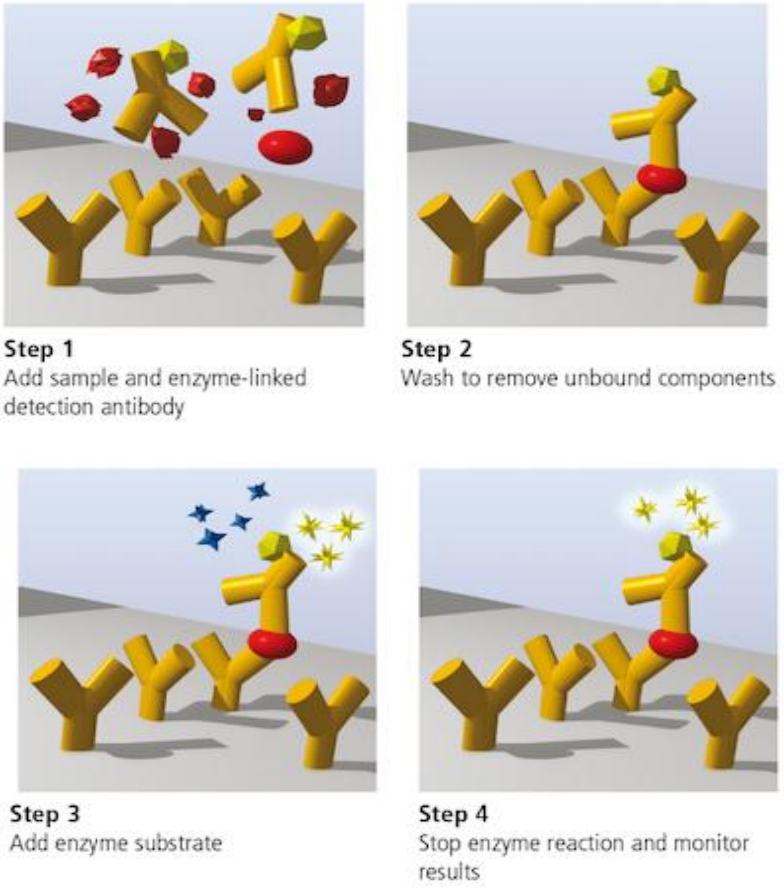

Figure 14. Overall ELISA mechanism: yellow Y on surface – capture antibody; floating yellow Y – detection antibody; red circle - insulin; blue stars - enzyme substrate; yellow stars - chromogenic signal[64]

The protocol for this assay begins by adding 25 µL of sample to a sample well which contains attached detection antibody. 100 µL of enzyme conjugate solution is then added and the plate incubated at room temperature for 1h. The plate is then washed to remove unbound components. The substrate is added and incubated at room temperature for 15 min. Finally, a stop solution is added and the color product measured at 450 nm. The working range of the assay is 3 – 200 mU/L so all samples were diluted to within this specified range.

3.2.3 FITC-labeled Insulin

Fluorescence was used to detect insulin for the characterization of the adjusted microbead model. Insulin was labeled with Fluorescein isothiocyanate (FITC) to track insulin release from the beads. The labeling procedure was adapted from a previously developed technique with minimal alterations[65]. FITC (1.75 mg) in 1 mL of DMSO was added to a solution of 35 mg insulin (10 mL) in 0.1 M Na_2CO_3. The FITC in DMSO was added to the insulin solution gradually in 40 separate aliquots in volumes of 25 μL. This solution was incubated at 4°C for 8 h, then 30 mL of 1 M NH_4Cl added and incubated at 4°C for an additional 2 h. Finally, the solution was dialyzed for 3 days with 3500 Da MWCO dialysis tubing to remove unbound label. The amount of FITC released over the course of the dialysis period was tracked to ensure all unattached label was removed from the insulin solution. The final labeled insulin solution was evaluated to determine the molar ratio of insulin bound to label.

3.3 Microparticle Model

3.3.1 Preparation

3.3.1.1 Insulin Loaded Before Gelation

Insulin was encapsulated in alginate beads formed through external gelation with calcium chloride based on a previously developed technique[32]. A 2% (w/v) alginate solution was combined with 1 mL Novolin ge Toronto insulin for every 10 mL alginate solution. The pH was adjusted to a range between 4.5 and 4.9 to ensure the insulin (pI 5.3) had a positive charge, promoting attraction to the negatively charged alginate. The

solution was extruded dropwise into 100 mM calcium chloride solution. An air jet was incorporated to impinge on the extrusion needle to aid in reducing the overall size of the beads. The formed beads were mixed in the calcium chloride for a short time to ensure stable formation. The microbeads were either used immediately or stored in 100 mM calcium chloride at 4°C.

3.3.1.2 Insulin Loaded After Gelation

The 2% alginate solution and blank beads were prepared the same way as described in the previous section except for the absence of insulin. Beads (5 g) were then submerged in an insulin solution with a concentration of 0.167 mg/mL (21 mL), 0.318 mg/mL (22 mL), or 0.583 mg/mL (24 mL) for 3h. Insulin uptake was tracked by analyzing supernatant and quantified with a micro-BCA assay. Insulin loaded beads were used immediately or stored in insulin solution at 4°C.

3.3.2 Characterization

Beads were evaluated based on their size, shape, Young's modulus, and insulin loading. Size and shape were investigated visually through images obtained with a Wild M3 optical microscope. Young's modulus was determined through the use of a texture analyzer with a 5 kg load cell. Individual beads were compressed until the point of collapse. A stress-strain curve was produced and Young's modulus was calculated based on the slope of the linear portion of the curve. Insulin loading was evaluated by dissolving the beads in a phosphate buffered saline (PBS) solution overnight, and then measuring released insulin with a micro-BCA assay. This measured amount was compared to a theoretical value based on how much insulin was initially added. Release

studies were performed in simulated GIT fluids without enzymes to evaluate the release kinetics of the alginate microbeads. Microbead samples (3 g) were suspended in 30 mL of release fluid. Beads were added to simulated gastric fluid without enzymes (USP31-NF26) for 1 h and then transferred to simulated intestinal fluid without enzymes (USP31-NF26) for 2 or 3 h. Supernatant samples were analyzed with a micro-BCA assay.

3.4 Nanoparticle Model

3.4.1 Preparation

Nanoparticles were prepared based on a previously described method based on the formation of a particle core through ionotropic gelation with added coatings through polyelectrolyte complexation[66]. A starting solution (117.5 mL) was prepared containing 0.063% (w/v) alginate, 0.039% (w/v) dextran sulfate, 0.037% (w/v) poloxamer 188, and 7 mg insulin. The solution was adjusted to a pH of 4.9 before 7.5 mL of 18 mM calcium chloride was added dropwise over the course of 60 min. The nanoparticle cores were coated in 0.04% (w/v) chitosan solution prepared in 0.04% (w/v) lactic acid solution. 25 mL of chitosan solution were adjusted with sodium hydroxide to a pH of 4.6 and then added dropwise to the nanoparticle suspension over a 90 min time period. Finally, the nanoparticles were coated with bovine serum albumin (BSA) at a pH of 5.1. 25 mL of 0.5% (w/v) BSA solution were added over a 60 min period. The nanoparticle suspension was constantly agitated via magnetic stirring at a rate of 800 rpm. The finished nanoparticles were stored in suspension at 4°C until use.

3.4.2 Characterization

The nanoparticles were evaluated based on their average diameter, particle mass per suspension volume, insulin loading, and encapsulation efficiency. Particle diameter was determined with a Zetasizer Nano ZS (Malvern Instruments Ltd.). A size distribution curve was developed based on dynamic light scattering from which the average diameter of the particle sample was calculated as a function of intensity (%). The particle suspension density was evaluated by measuring the amount of solid particle mass in a specific volume of total nanoparticle solution as follows. The nanoparticle suspension (20 mL) was centrifuged at 20,000 g for 1h. The mass of the wet pellet formed was measured, and the ratio of solid particle mass to suspension volume was calculated. Insulin loading and encapsulation efficiency were evaluated by dissolving a sample of nanoparticles in a solution of 0.1 M PBS and 0.1 M EDTA over the course of 48 h. After 24 h, the particles were separated through centrifugation and re-suspended in fresh buffer to ensure all the insulin was released. At the end of 48 h, insulin released after each 24 h period was quantified using a human insulin ELISA. This measured value was compared to a theoretical value based on the initial amount of insulin added when forming the nanoparticles.

3.5 Adjusted Microbead Model

3.5.1 Preparation

The adjusted microbead system was developed as a simplified way to evaluate the interactions of the formulation components of the nanoparticle model. The particles in

the nanoparticle system pose challenges related to handling and transfer since they cannot be visualized with the naked eye. The adjusted microbeads simplify handling and transfer procedures since they are significantly larger and easy to see. This system was optimized in terms of solid concentrations, calcium chloride concentration, and extrusion rate. The beads were formed through external gelation similar to the method used in producing the simple microbeads discussed in section 3.3. A solution of alginate, dextran sulfate, poloxamer 188, and insulin was added drop-wise under an air jet to calcium chloride. There were two formulations for the core solution: 0.063% (w/v) alginate, 0.039% (w/v) dextran sulfate, and 0.037% (w/v) poloxamer 188 and 2% (w/v) alginate, 1.24% (w/v) dextran sulfate, and 1.17% (w/v) poloxamer 188. Two concentrations of calcium chloride were investigated: 18 mM and 100 mM. Five different extrusion rates were applied: 0.125, 0.25, 0.5, 1, 2 mL/min. All combinations of conditions were attempted in order to determine an optimal formulation. Optimization was based on the formation of discrete, stable beads at the smallest size possible. The optimized beads were coated with chitosan and BSA. Beads were agitated in 0.04% (w/v) chitosan solution for 1h and then transferred to 0.5% (w/v) BSA solution for an additional hour. After the final coating, the adjusted microbeads were either used immediately or stored in 0.5% (w/v) BSA solution at 4°C.

3.5.2 Characterization

The adjusted microbeads were examined visually with the aid of an M3 optical microscope to evaluate the general shape of the beads and their average size. Insulin loading was determined by dissolving a sample of the beads in 0.1 M PBS and 0.1 M EDTA. Insulin was quantified through either fluorescence of FITC-labeled insulin or

ELISA. A release study was performed where 0.5 g of beads were added to 10 mL of simulated gastric fluid or simulated intestinal fluid (USP31-NF26) without enzymes for 2 h. Supernatant samples were detected for insulin using a human insulin ELISA for gastric conditions and fluorescence of FITC for intestinal conditions. The ELISA was necessary due to insulin degradation observed in simulated gastric fluid. Fluorescence of FITC would not be able to detect changes in insulin conformation since the label will always be present.

3.6 Physical Modeling

Two physical models for *in vitro* testing were compared: an actively mixed simulator and a passively mixed simulator. The actively mixed simulator design is based on the usual technique applied for *in vitro* release investigations in small lab settings. The system consists of a small flask and stir bar which is agitated at a rate of 100 rpm. Relatively slow mixing is applied in an attempt to mimic the gentle mixing of the GIT. The passively mixed simulator designed for this study consisted of a 500 mL Tedlar bag with septum port used for filling and sampling representing the volume of the stomach. The passively mixed simulator was agitated on a Roto-Shake Genie at a rate of 10 cycles per minute and an angle of 10°. The vertical displacement of the bag at the ends furthest from the axis was roughly 13 mm. Two attachments are available for the Roto-Shake device: a rocking system and a rotating system. A diagram of both models is shown in **Figure 15**.

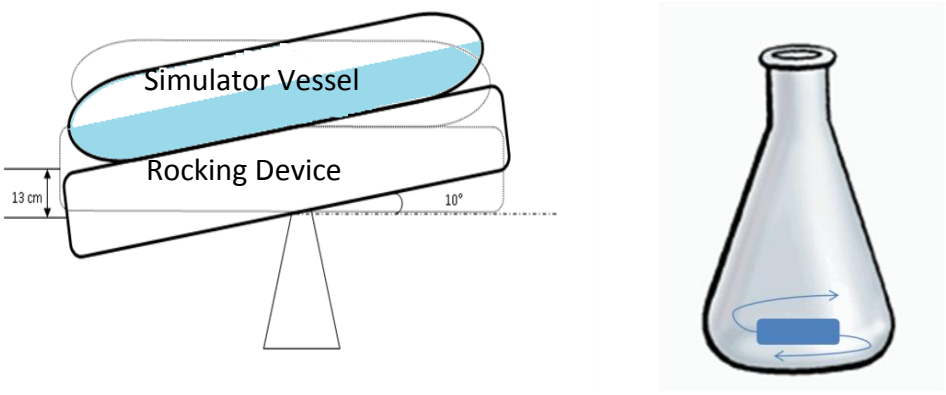

(a) (b)

Figure 15. Physical model systems: (a) passively mixed simulator (b) actively mixed simulator

3.7 Physical Model Testing

3.7.1 Mixing Characteristics

The mixing characteristics of the simulator systems were evaluated through a pH tracer tracking study. The actively mixed simulator and both attachments for the passively mixed simulator were evaluated. In addition, the response of the pH probe was determined to evaluate its time constant. Vessels were filled with 200 mL of distilled water and 0.5 mL of 1 M HCl added as tracer. The pH was recorded every 5 sec until stable. Differences in response time were evaluated to determine differences in the mixing patterns.

3.7.2 *In vitro* Release with Microbeads

An *in vitro* release was performed with the microbead drug delivery model. To begin, vessels were filled with 200 mL of simulated gastric medium without enzymes at pH 1.7 (USP31-NF26) together with 17 g of wet microbeads. The microbeads were agitated in gastric conditions for 60 min before being transferred into 200 mL of simulated intestinal fluid without enzymes at pH 7.4 (USP31-NF26) for an additional 100 min. Supernatant samples were collected throughout the total release time and sample volume replaced with the same volume of fresh GI fluid. The insulin released was quantified using a Micro-BCA assay.

3.7.3 *In vitro* Release with Nanoparticles

In vitro release was examined with the nanoparticle model system with slight modifications to the procedure for the microbead system. 100 mg of nanoparticles (20 mL nanoparticle suspension) were added to 100 mL of simulated gastric fluid without enzymes (USP31-NF26) in both simulator vessels. After 120 min, the nanoparticles were separated from the gastric fluid by centrifugation at 20,000 g for 15 min. The separated particles were re-suspended in 100 mL of simulated intestinal fluid without enzymes (USP31-NF26) for 180 min. Samples were collected (1 mL) throughout the time of the release, replacing the volume with the appropriate GI fluid. All samples were centrifuged at 20,000 g for 15 min before insulin quantification to remove any particle debris. Insulin concentrations were measured with a human insulin ELISA.

3.7.4 *In vitro* Release with Adjusted Microbeads

An *in vitro* release was performed with the adjusted microbeads in simulated gastric fluid. Beads (2.5 g) were added to 50 mL of simulated gastric fluid without enzymes (USP31-NF26) in the passively mixed simulator for 2 h. Supernatant was sampled throughout the 2 h release and insulin was quantified with a human insulin ELISA. Results were compared to those achieved with the actively mixed simulator.

3.8 Fluid Model Testing

3.8.1 Trypsin

Trypsin was chosen as a model enzyme found in intestinal fluid. Chymotrypsin and other carboxypeptidases are also present in physiological intestinal fluid. The effects of trypsin on the stability of insulin within the nanoparticle system were tested.

3.8.1.1 Insulin Degradation by Trypsin

Trypsin was first evaluated with free insulin to ensure that insulin breakdown was significant within a reasonable amount of time and that it would be detectable by the human insulin ELISA. Novolin ge Toronto insulin was subjected to trypsin degradation for either 1 or 2 h. The results were compared to insulin samples prepared without enzyme. Insulin solution and trypsin solution were prepared with the same molar concentration (0.06 μM) based on a previously reported study[67]. A solution of trypsin inhibitor was prepared that was the same mass concentration as the trypsin solution (0.0014 mg/mL) since 1 mg of trypsin inhibitor will react with 1 mg of trypsin[68]. Both the trypsin and the inhibitor were dissolved in Tris buffer. The insulin samples without

enzyme were prepared with 10 mL of Tris buffer and 5 mL of 0.06 μM insulin solution. The insulin samples with enzyme were prepared with 5 mL of 0.06 μM trypsin in Tris solution and 0.06 μM insulin solution. At the end of 1 or 2 h, 5 mL of 0.0014 mg/mL trypsin inhibitor solution were added and mixed for 30 min to stop the reaction of the trypsin. Control samples of Tris alone and Tris with trypsin and trypsin inhibitor were prepared to evaluate any possible interactions with the ELISA during insulin quantification. All samples were agitated at 100 rpm at 37°C for the duration of the test period. Insulin quantification was performed with a human insulin ELISA. The differences in measured insulin between the samples with and without trypsin were evaluated.

3.8.1.2 Effects on Nanoparticle Model

The effects of trypsin on a drug delivery model were tested with the nanoparticles. Nanoparticle samples were prepared with and without trypsin for time points of 1, 2, and 5 h. Samples without trypsin were prepared with 4 mL of Tris buffer and 2 mL of nanoparticle suspension, corresponding to roughly 15 mg of nanoparticles. Samples with trypsin were prepared by combining 2 mL (15 mg) of nanoparticle suspension and 2 mL of 6.9 μM trypsin in Tris buffer. After the specific time period, 2 mL of 0.16 mg/mL trypsin inhibitor solution were added and mixed for 30 minutes. At the end of the experiment, all nanoparticle samples were dissolved with a solution of 0.1 M PBS and 0.1 M EDTA to determine the amount of intact insulin retained inside the particles. Samples were agitated at a rate of 100 rpm at 37°C. All insulin was quantified through the use of a human insulin ELISA. Differences between insulin retained in nanoparticles exposed to trypsin and not exposed to trypsin were evaluated.

3.8.2 Pepsin

Pepsin was applied as a model enzyme found in physiological gastric fluid. The addition of pepsin was used to evaluate drug device stability in simulated gastric conditions with enzymes.

3.8.2.1 Insulin Degradation by Pepsin

The degradation of fresh insulin by pepsin was evaluated in a study similar to the trypsin validation. Pepsin with an activity of 2190 U/mg was added to simulated gastric fluid (USP31-NF26) at a concentration of 50 U/mL. Pepsin was inactivated through the addition of 0.005 mg/mL pepstatin A in ethanol. Insulin samples with and without pepsin were compared at two time points: 1 and 2 h. To begin, 5 mL of insulin solution were added to 5 mL of gastric fluid (with or without pepsin). At the end of each time point, 5 mL pepstatin A in ethanol were added to each sample and mixed for 30 min. Samples were mixed at 100 rpm in a water bath at 37°C. Insulin was quantified with a human insulin ELISA to compare amounts of intact insulin present when exposed to gastric fluid with and without pepsin.

3.8.2.2 Effects on Adjusted Microbead Model

The effects of pepsin were evaluated with the adjusted microbead delivery system in the actively mixed and passively mixed simulators. In the actively mixed simulator, insulin loaded beads (0.5 g) were added to 10 mL of simulated gastric fluid with and without pepsin at a concentration of 50 U/mL. One set of samples was mixed for 30 min

in gastric fluid before pepsin was added. In this case, 0.5 g of beads were suspended in 10 mL of simulated gastric fluid without pepsin. After 30 min, 10 mL of simulated gastric fluid containing 50 mU/L of pepsin were added. All samples were agitated at a rate of 100 rpm in a water bath at 37°C. In the passively mixed simulator, beads (2.5 g) were added to 50 mL simulated gastric fluid with and without pepsin (50 U/mL). The time points studied were 1 and 2 h. At the sample point, the gastric fluid (with or without pepsin) was removed and 0.005 mg/mL pepstatin A in ethanol added to inactivate pepsin if it was present. 10 mL were added to the actively mixed simulator and 50 mL were added to the passively mixed simulator. These solutions were mixed for 30 min before beads were dissolved in a solution of 0.1 M PBS and 0.1 M EDTA at 800 rpm. The final solutions were sampled and analyzed for insulin content using a human insulin ELISA. The amount of insulin retained within the particles was compared between samples that were, or were not exposed to pepsin degradation.

3.8.3 Simulated Intestinal Buffers

Different simulated intestinal buffers were evaluated using the adjusted microbead model. Three buffer formulations were used: standard phosphate buffer, standard Kreb's bicarbonate buffer, and Kreb's bicarbonate buffer with a 1:1 NaCl:$CaCl_2$ ratio. The specific components in each buffer are detailed in **Table 5**.

Table 5. Components of simulated intestinal buffers

Components (mM)	**Standard Phosphate Buffer**	**Standard Kreb's Bicarbonate Buffer**	**Kreb's Bicarbonate Buffer (1:1 NaCl:$CaCl_2$)**
KH_2PO_4	1.8	1.2	1.2
Na_2HPO_4	10	–	–
$NaHCO_3$	–	24	24
NaCl	–	118	60
KCl	–	4.7	4.7
$CaCl_2$	–	2.5	60
$MgSO_4 \bullet 7H_2O$	–	1.2	1.2

Adjusted microbeads (2.5 g) were added to 50 mL of intestinal buffer in the rotating passively mixed simulator for 150 minutes. Supernatant was sampled and insulin was quantified with ELISA. The release profiles for each intestinal buffer was evaluated and compared.

Chapter 4: Results and Discussion

4.1 Assay Development

Each drug delivery device formulation has different components and properties that require different analytical techniques to accurately measure the insulin present. As a result, three different assay methods were applied to quantify insulin in different circumstances. The following is a discussion on insulin assay development for the Micro-BCA assay, human insulin ELISA, and fluorescent labeling.

4.1.1 Micro-Bicinchoninic Acid (BCA) Assay

Quantification of insulin in the microbead model was performed using a Micro-BCA protein assay. The assay is based on the reduction of Cu^{2+} to Cu^{1+} by proteins. Bicinchoninic acid will react with Cu^{1+} forming a purple complex which is quantified to determine the amount of protein present[63]. A calibration plot is produced using varying concentrations of insulin. An example is shown in **Figure 16**.

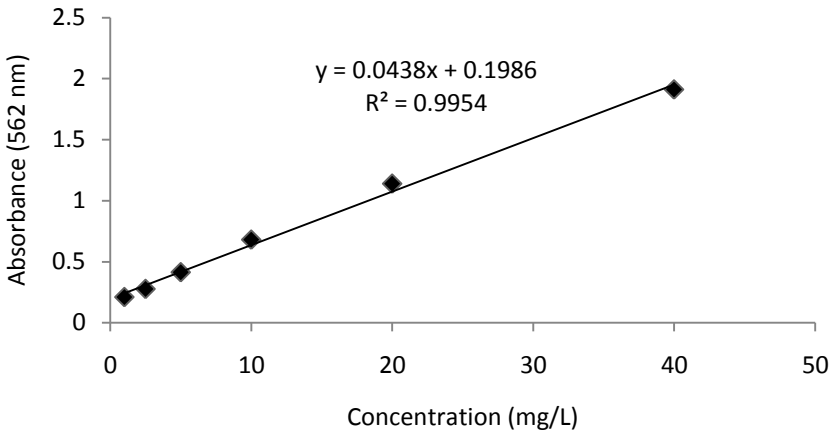

Figure 16. Micro-BCA insulin standard curve

All samples containing unknown amounts of insulin were diluted until they were in the calibration range (2 – 40 mg/L). This assay was only used for the microbead model since it was discovered that there was interference with alginate. Interference was particularly noticeable when microbeads were dissolved to measure retained insulin. Assay results in the presence of soluble alginate tended to be unusually high indicating higher than expected insulin quantities present in samples. Other concerns came up when working with the nanoparticles and adjusted microbeads since both formulations contained bovine serum albumin (BSA) which will give a positive reading with the BCA assay, thus other assay methods were applied.

4.1.2 Human Insulin ELISA

A human insulin ELISA (enzyme linked immunosorbent assay) was used to measure insulin in the nanoparticle model and adjusted microbead model. This is a sandwich ELISA simultaneous assay based on binding the insulin between two different antibodies. The insulin binds to the capture antibody in the plate well and subsequently with the

detection antibody. This binding is quantified by the addition of a substrate which reacts with the enzyme, linked to the detection antibody, producing a chromogenic signal that is measured spectrophotometrically. The use of the ELISA was necessary to avoid complications with the micro-BCA assay due to the presence of BSA in the nanoparticle and adjusted microbead structures, and to avoid alginate interference. Two different standard curves were developed to ensure an accurate reading of the insulin. One curve was based on standard human recombinant insulin solutions supplied with the ELISA kit. This was compared to a plot based on solutions of Novolin ge Toronto human recombinant insulin, which was used in the nanoparticle preparation. Samples at each concentration were prepared and measured twice at 450 nm. The insulin concentrations were averaged, and the standard deviation is represented by the error bar. The results of this comparison are depicted in **Figure 17**.

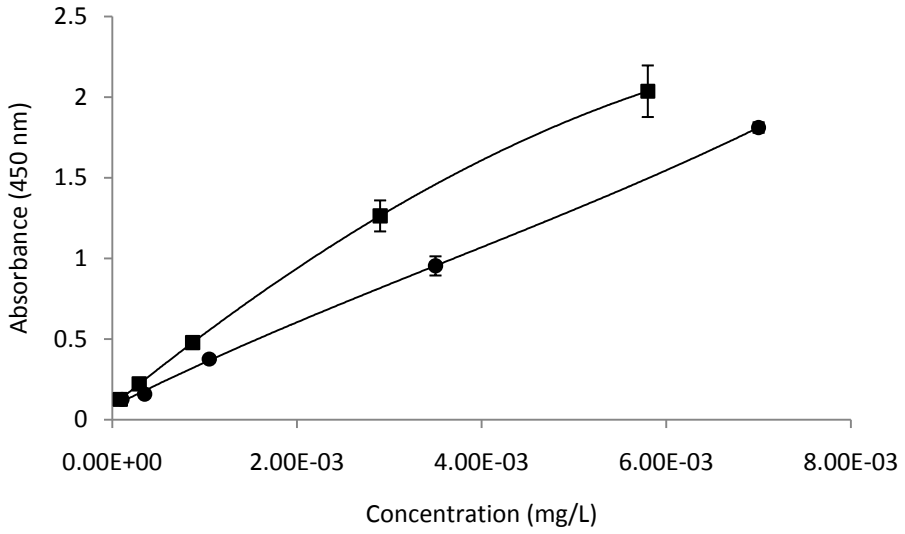

Figure 17. Human insulin ELISA calibration plots using insulin standard solutions provided with the commercial assay kit (■) and Novolin ge Toronto insulin which was used in the present study (●)

It is seen that the two calibration plots were similar. Differences between the two plots are more noticeable at higher concentration values. The human insulin ELISA is a sensitive assay that detects and quantifies low quantities of insulin at concentrations of $1.16 \times 10^{-4} - 5.80 \times 10^{-3}$ mg/L, so all unknowns were diluted to an appropriate concentration for accurate detection. The error bars are small indicating that the assay is very repeatable. ELISA will detect only intact insulin since it is based on the detection antibody binding to the whole insulin molecule. Other assays will not be able to detect whether the insulin is in its full molecular form or if any breakdown has occurred.

4.1.3 FITC-labeled Insulin

Fluorescent label was used to quantify insulin during the characterization of the adjusted microbead model. This method was chosen to avoid interactions associated with the Micro-BCA assay and the large dilutions necessary to quantify insulin using ELISA. In addition, ELISA is an expensive assay, so is reserved for when alternatives are not appropriate. FITC was used to label insulin and track its release from the delivery device. Previous studies have used excitation wavelengths between 480 and 495 nm for FITC analysis[69] [70] [71] [72]. Appropriate excitation and emission wavelengths were determined for this system. Samples of FITC in water were excited at 490 nm with a cutoff of 495 nm. Emission wavelengths were tested between 360 and 750 nm. The results are shown in **Figure 18.**

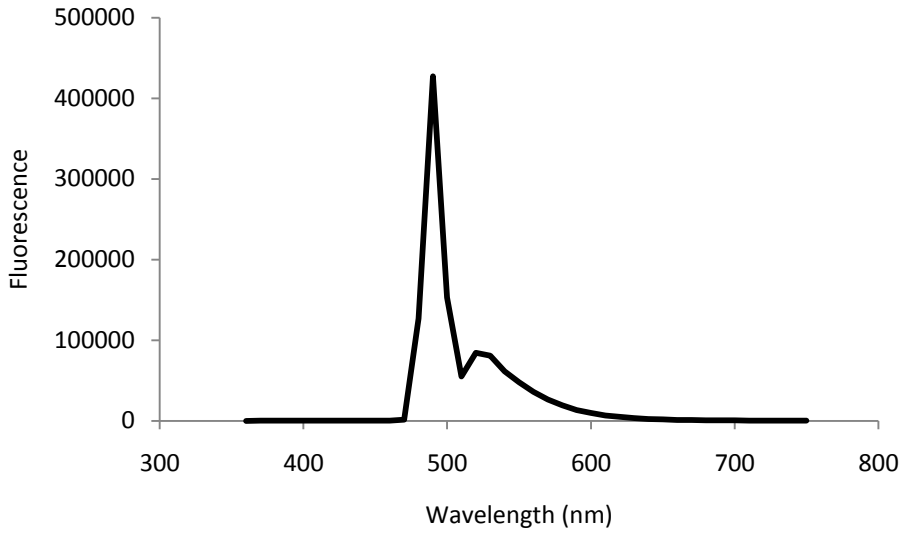

Figure 18. Evaluation of appropriate FITC emission wavelength for excitation at 490 nm

The smaller peak indicates an emission wavelength near 520 nm. The wavelengths for excitation and emission were chosen to be 490 nm and 520 nm, respectively. These wavelengths were used in all subsequent analysis of FITC labeled insulin samples. A calibration curve was developed to track quantities of the FITC label and is shown in **Figure 19**.

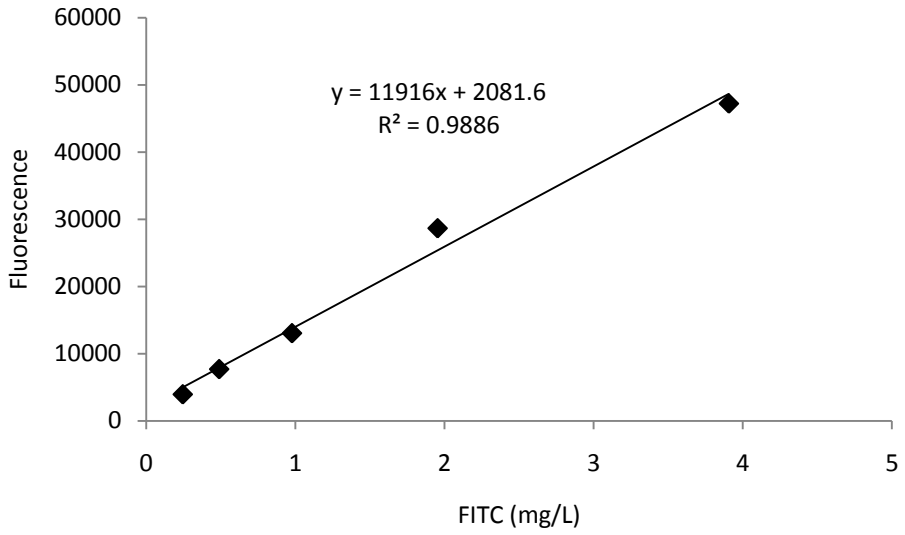

Figure 19. FITC calibration curve: excitation – 490 nm, emission – 520 nm

The linear reading range is between 0.2 and 4 mg/L of FITC. Higher concentrations of FITC led to decreased emission, likely due to an increasing absorbance effect of the FITC. Samples of insulin-FITC were then serially diluted beyond the calibration range to ensure that the fluorescence readings fall within the calibration range.

A calibration curve was also developed for FITC-insulin. The measurable concentration range was between 2 and 600 mg/L as shown in **Figure 20**.

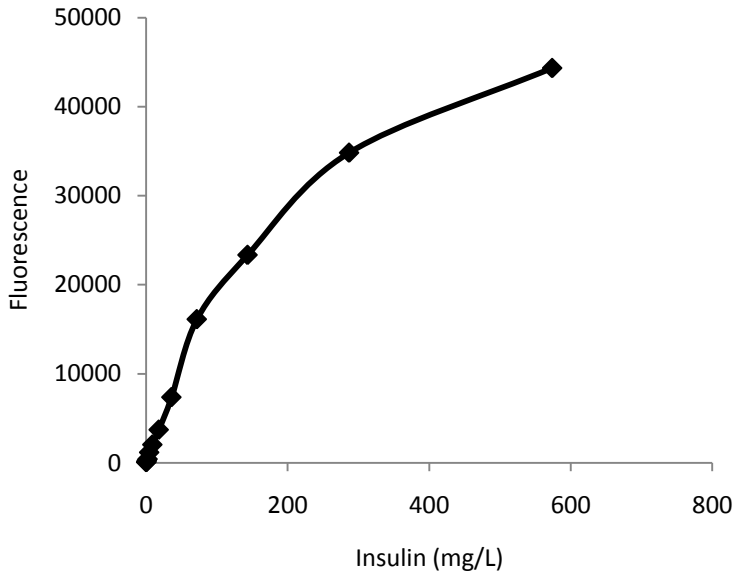

Figure 20. FITC-insulin calibration plot (excitation – 490 nm, emission – 520 nm)

A linear fit of the data was used for analysis of insulin concentrations between 0 and 143 mg/L while a second order polynomial fit was used for insulin concentrations of 143 – 573 mg/L. FITC-labeled insulin was dialysed for 72 h and the amount of unattached FITC released was tracked. After ensuring that all label present was attached to insulin, the amount of insulin:FITC was determined. The molar ratio of insulin to FITC was 2.15, indicating that one FITC was bound for every 2.15 molecules of insulin.

4.2 Drug Delivery Device Development

Three drug delivery device models were formulated to evaluate the different components of *in vitro* GIT modeling, including a microbead model, nanoparticle model, and an adjusted microbead model. The basic characteristics and qualities defining these models are discussed in the following sections.

4.2.1 Microbead Model

The microbead model was formed by encapsulating insulin in an alginate bead through air jet facilitated droplet extrusion. Droplets were captured in a calcium-based crosslinking solution resulting in gelation of the alginate using an external form of the calcium ion crosslinker. The insulin was incorporated into the alginate solution prior to gelation. An image of a typical batch of microbeads is shown in **Figure 21**.

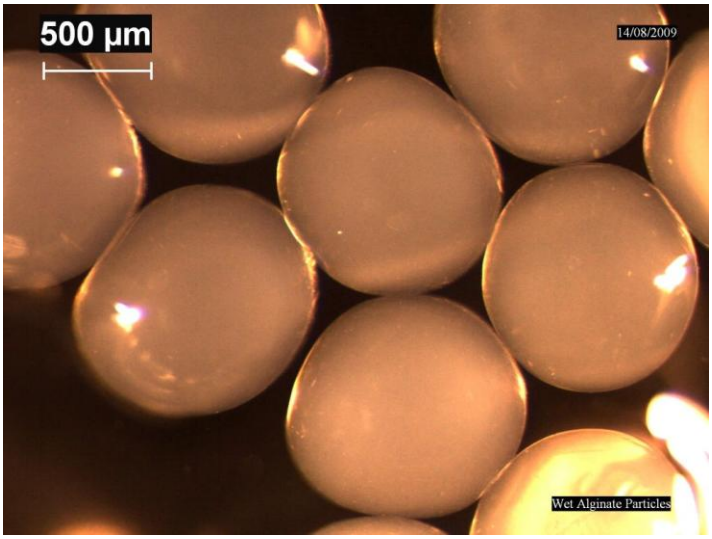

Figure 21. Wet alginate microbeads

The microbeads were generally spherical and uniform in shape with a size range between 700 and 1000 µm and a Young's modulus around 14.2 kPa. Numerous (9) batches of microbeads were prepared and the insulin loading determined by dissolving the beads in 0.1 M PBS solution, and assaying released insulin by Micro-BCA assay. Insulin loading was determined to be 0.11 ± 0.05 mg insulin/g beads. A release study was performed where 3 g of beads were suspended in 30 mL of gastric fluid for 1 h and then transferred

to 30 mL of intestinal fluid for 3 h. Released insulin was quantified with a Micro-BCA assay and the results are shown in **Figure 22**.

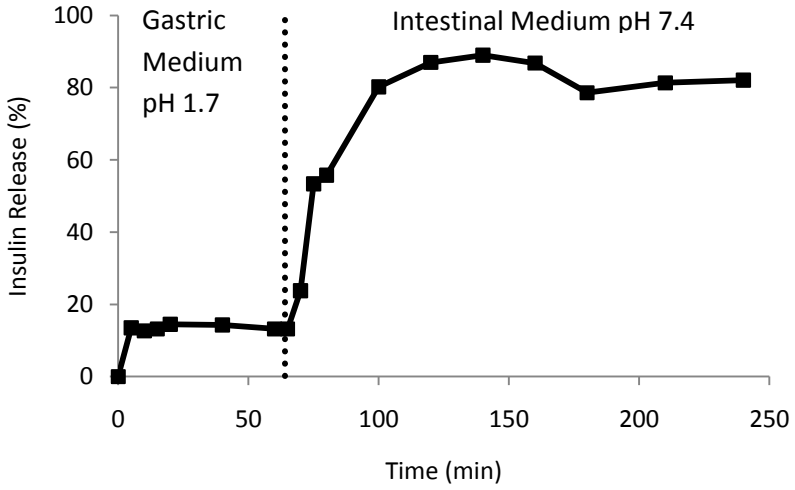

Figure 22. Insulin release from microbeads in simulated gastric fluid and simulated intestinal fluid without enzymes (USP31-NF26)

Less than 15% of the encapsulated insulin was released in the gastric fluid, and that release took place within the first 5 min. Most of the insulin is then retained due to the beads collapsing in acid, causing the structure of the beads to be less permeable. Alginate will protonate and collapse resulting in bead shrinkage under the low pH conditions of the gastric fluid[73]. This forms an insoluble and less permeable alginic acid particle that limits the release of encapsulated materials[74]. Insulin is then again released once the beads are transferred to intestinal fluid since the neutral pH results in a swelling of the beads, leading to a more permeable bead matrix. The alginic acid formed under gastric conditions will become increasingly soluble and thus unstable, enabling release of encapsulated insulin[74].

The size of the microbeads was measured in calcium chloride, gastric fluid, and intestinal fluid (bicarbonate buffer) to evaluate the effects of these different conditions further. The results are shown in **Figure 23**.

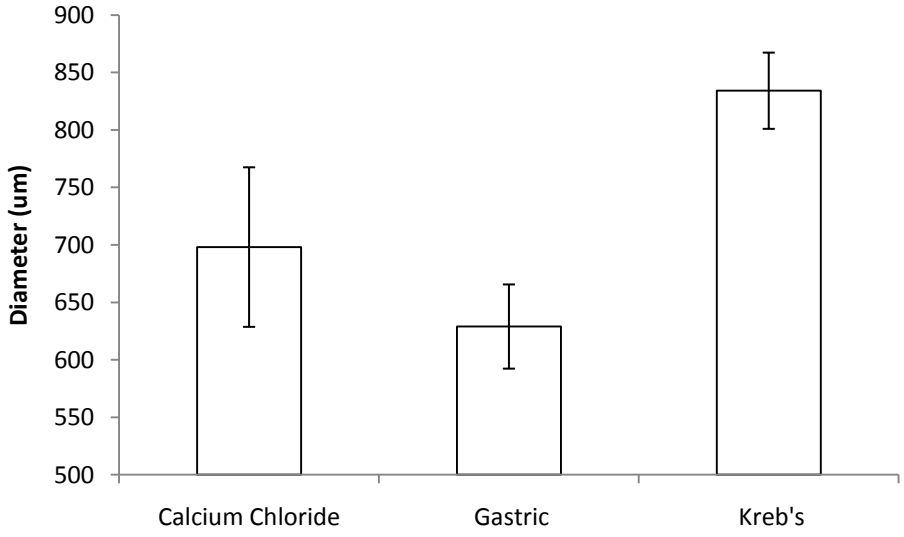

Figure 23. Average size of microbeads: (A) beads in $CaCl_2$ solution; (B) beads in gastric fluid; (C) beads in intestinal fluid (Kreb's bicarbonate buffer). Data represent means and standard deviations of diameters of 6 to 14 beads for each category.

The average diameters were 698 μm in $CaCl_2$, 629 μm in gastric fluid, and 834 μm in intestinal fluid, which correspond to average bead volumes of 0.178, 0.130, and 0.304 mm^3 respectively. This represents a 27% reduction in bead volume upon addition to gastric conditions, followed by a 2.3 fold increase in volume with subsequent addition to neutral pH based Kreb's buffer. The collapse of beads in gastric fluid is thought to aid in insulin retention within the beads and thereby protect the insulin from the GIT. As the beads swell in intestinal fluid, insulin is released from the bead network more easily.

Higher insulin loading was achieved by suspending blank microbeads in insulin solutions. The resulting diffusion of insulin into blank alginate microbeads was thus the

mechanism of bead loading. Beads (5 g) were submerged in solutions with varying insulin concentrations to examine the extent of insulin loading and resulting release. **Figure 24** shows the loading of insulin into beads.

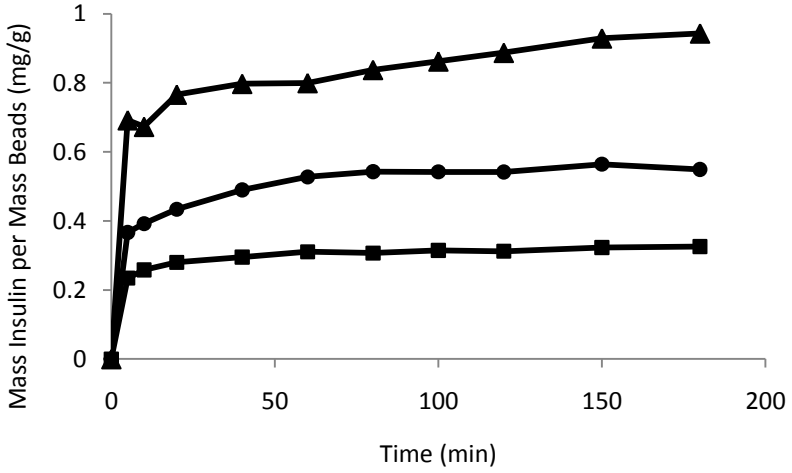

Figure 24. Insulin concentration in microbeads with solution concentrations of 0.167 mg/mL (■), 0.318 mg/mL (●) and 0.583 mg/mL (▲)

The final concentration of insulin in beads is compared to the concentration of insulin remaining in solution in **Table 6**. The concentration in the beads was evaluated by estimating the volume of beads present in a specific mass sample. The density of the beads was assumed to be the same as water (1 g/mL) for the purpose of this calculation.

Table 6. Insulin concentrations after loading into microbeads

Starting insulin concentration in loading solution (mg/mL)	Final insulin concentration in microbeads (mg/mL)	Final insulin concentration in solution (mg/mL)
0.167	0.326	0.093
0.318	0.548	0.213
0.583	0.949	0.463

In all cases, the concentration of insulin is higher in the microbeads than it is in the solution indicating a preference for the insulin toward the bead phase. The pH values of the alginate solution used to form the beads and the insulin loading solution had been adjusted to a range between 4.5 and 4.9. Insulin has a net positive charge (pI = 5.3 – 5.35[75]) and alginate is negatively charged (pKa 3.38-3.65[76]) at this pH, resulting in attraction between the insulin and the alginate polymer, promoting uptake. In addition, uptake of insulin occurs very rapidly. Most uptake occurs within the first few minutes after the beads are suspended in the insulin solutions, indicating that the microbeads are very permeable to the insulin and allow for rapid diffusion to occur into the bead phase.

Insulin release from the beads was then examined in acidic simulated gastric fluid for 1h, then in neutral pH intestinal fluid for 2h. Microbeads (3 g) were added to 30 mL of release fluid and supernatant was sampled throughout the entire release. Insulin in supernatant was evaluated with a Micro-BCA assay and results are shown in **Figure 25**.

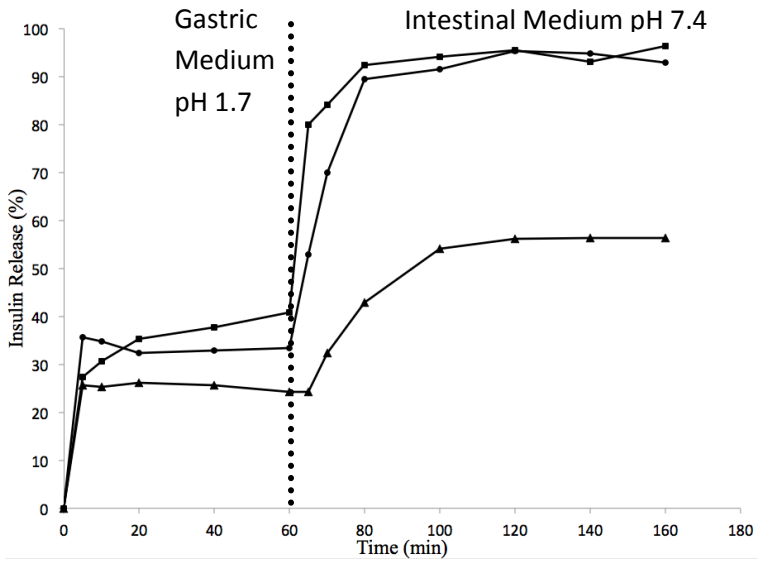

Figure 25. Release profiles for beads loaded with insulin through absorption mechanism. Initial insulin concentration in beads was 0.326 mg/mL (■), 0.548 mg/mL (●) and 0.949 mg/mL (▲))

Insulin from beads at the three different loadings, all show a similar trend in the gastric fluid where 25-35% of the insulin was released within the first 5 minutes, and then no further release was observed for the remaining period of 60 min. Once the beads were transferred to intestinal fluid, 90% of the insulin was released after 20 min for beads with insulin concentration of 0.326 mg/mL and 0.548 mg/mL. Only 50% of the insulin was released for the beads with insulin concentration 0.949 mg/mL. The release profile for these beads with the highest loading of insulin was repeatable (data not shown), but is inconsistent with the other batches where most insulin was released in intestinal conditions.

From these results, it is seen that the alginate microbeads are permeable to insulin diffusion. The insulin appears to have a strong attraction to the alginate beads as shown

in Table 6 where there is a higher concentration of insulin in the bead phase compared to the insulin solution phase at the end of the loading period. This is likely due to charge effects caused by the pH of the alginate and insulin solutions. The release profile for the beads loaded by absorption (Figure 25) was compared to that for the beads that were loaded with insulin before gelation (Figure 22). The initial release in gastric fluid was noticeably greater for the beads loaded by absorption where all three trials released at least 25% of the insulin within the first 5 minutes. This is compared to the microbeads discussed in section 4.2.1 with insulin added to the alginate solution before beads were formed through gelation, where only 13% of the insulin is released in gastric fluid. This difference may be due to the way the insulin is incorporated within the bead. The beads loaded by absorption could have more insulin near the surface of the bead facilitating subsequent release. The insulin within the beads loaded before gelation might be better dispersed throughout the alginate matrix of the bead helping to prevent some release. This comparison is similar in intestinal fluid as well except for the beads loaded through absorption with the highest concentration of insulin. The beads loaded before gelation release 80% of insulin after 40 minutes in intestinal fluid, while the batches loaded through absorption for the two lower concentrations of insulin released 80% after only 20 minutes. This again could be due to insulin being nearer to the surface for the beads loaded by absorption allowing insulin to be released more easily.

4.2.2 Nanoparticle Characterization

The nanoparticle model was formulated based on ionotropic gelation of a particle core consisting of alginate, dextran, poloxamer, and insulin followed by coatings through polyelectrolyte complexation with chitosan, then by BSA. Calcium chloride (7.5 mL)

was added drop-wise to 117.5 mL of a mixed solution containing 0.063% alginate, 0.039% dextran sulfate, 0.037% poloxamer, and 7 mg insulin over the course of 1h. The formed particles were coated with 25 mL 0.04% chitosan solution through drop-wise addition over 90 min, followed by 25 mL 0.5% BSA through drop-wise addition over 1h. The nanoparticles were characterized based on size, mass of particles in the suspension, and insulin loading and encapsulation efficiency. Size was evaluated with a zetasizer which produces a size distribution plot based on dynamic light scattering to measure Brownian motion, which is related to particle size by measuring intensity fluctuations of scattered light[77]. The motion of the particles is related directly to size with larger particles moving more slowly than smaller particles. **Figure 26** displays a typical result for the diameter distribution in nm (d. nm) of the nanoparticles based on intensity of the scattered light.

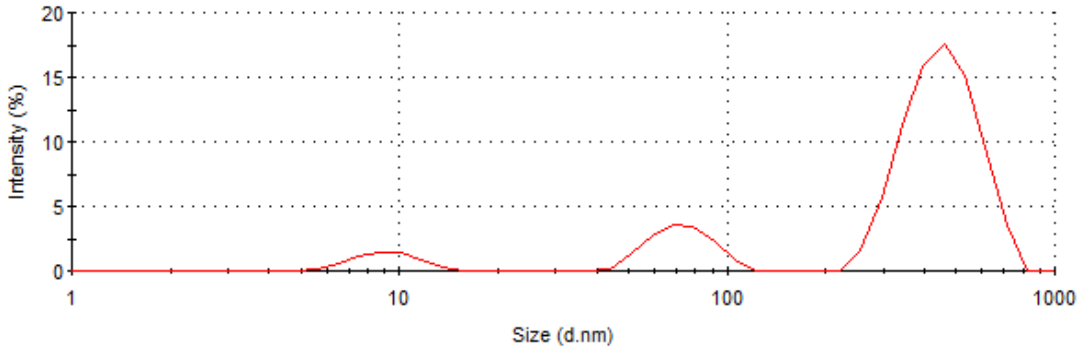

Figure 26. Diameter distribution of nanoparticles in nm (d. nm)

For each batch, 2 samples were evaluated by the zetasizer, which reads each sample 4 times. In the example in Figure 26 these measurements resulted in a mean diameter of 460 nm. Small intensity peaks indicate particles with diameters below 100 nm. The distribution of mean diameters ranged between 400 and 600 nm for six individual batches

of nanoparticles. A SEM image from previously reported results of a representative nanoparticle is shown in **Figure 27** displaying a particle that is both relatively smooth and spherical.

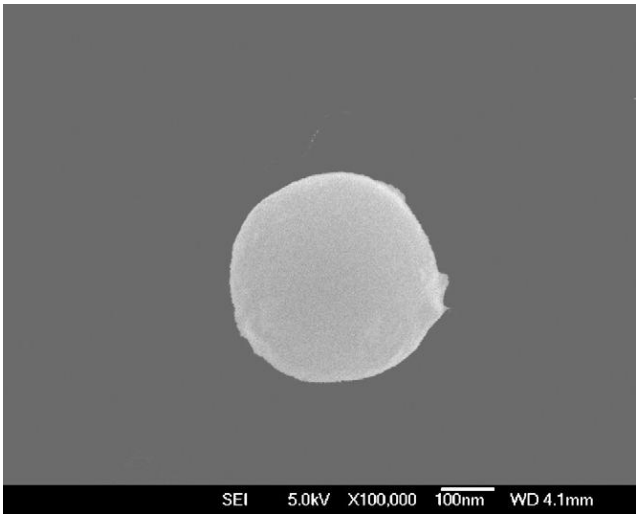

Figure 27. Image of representative nanoparticle[44]

Six batches of nanoparticles were prepared and the quantity of particles/volume nanoparticle suspension determined. Nanoparticles were handled as a liquid suspension since separation techniques are difficult and often encourage aggregation of particles. The mass of the nanoparticles in a volume of suspension averaged 7.4 ± 1.8 mg/mL. The average insulin loading was 3.94 ± 1.31 mg insulin/g particles, corresponding to an encapsulation efficiency of 72.6 ± 21.2%. This nanoparticle formulation was developed previously by a co-researcher[66]. The previously reported mean diameter for this formulation was 400 nm which coincides well with the diameter determined here of 460 nm. The encapsulation efficiency was reported previously as 100%. The encapsulation

efficiency reported here is less but within a reasonable range considering the error in the measured value.

A release study was performed previously where 10 mg of nanoparticles were suspended in 10 mL of release buffer[44]. Particles were agitated with a magnetic stir bar at 100 rpm for 2 h in gastric fluid and 3 h in intestinal fluid, both without added enzymes. Insulin release was measured using HPLC. The results are shown in **Figure 28**.

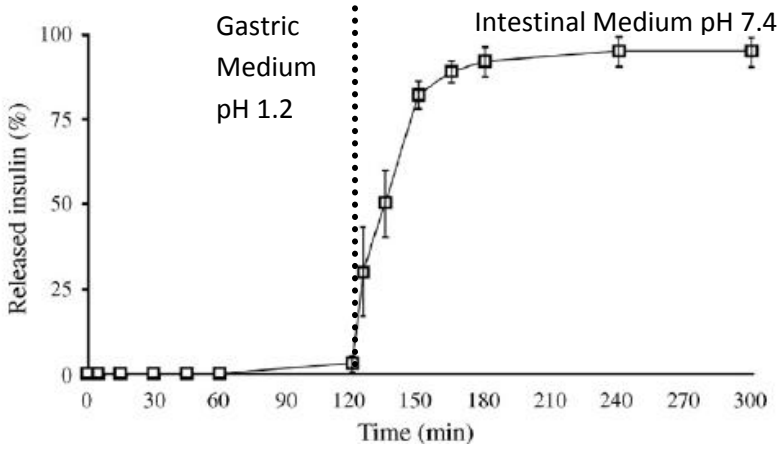

Figure 28. Insulin release profile for nanoparticles in gastric fluid followed by intestinal fluid[44]

Little release is seen over the first 2 h while the particles are exposed to the acidic gastric fluid. The particles appear to become impermeable in acid and limit the release of insulin into the supernatant. Following transfer to intestinal fluid, all insulin was released after 1h. The neutral conditions cause the polymer matrix to swell and become more permeable facilitating insulin release. These results are similar to what was seen with the microbead model in Figure 22, where most of the insulin is retained in gastric fluid but is quickly released when beads are transferred to intestinal fluid.

Insulin was tracked with the nanoparticles in gastric fluid to account for insulin that is either released or retained within the particle. Particles were immersed in simulated gastric fluid without enzyme at room temperature. Supernatant was sampled to determine the amount of insulin released. In addition, particles were sampled at the same time points, dissolved and released insulin assayed with ELISA. The results for the nanoparticle system are shown in **Figure 29**.

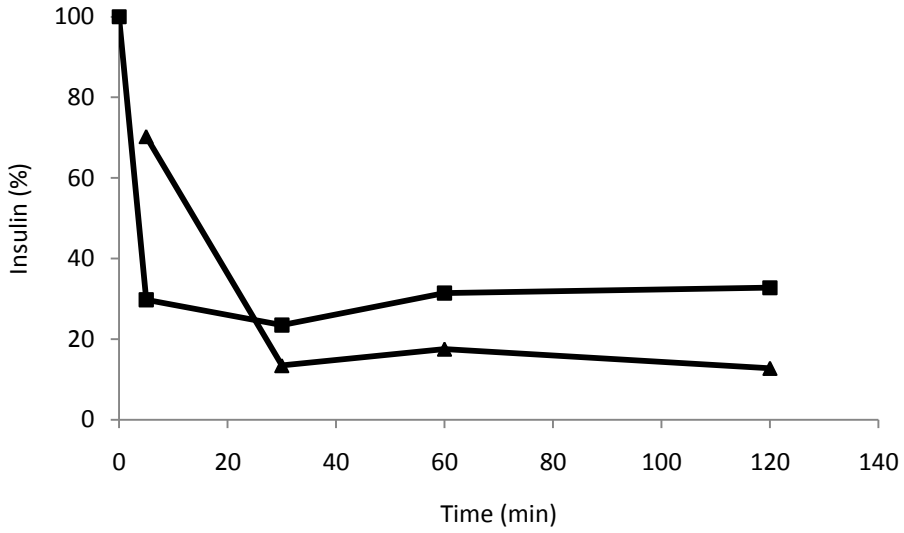

Figure 29. Insulin tracking for nanoparticles in gastric fluid: retained insulin (■), released insulin (▲)

Initially, all of the insulin is within the nanoparticles, but after addition to the simulated gastric medium, there was an immediate release. Following this initial release, 70% of the insulin is seen retained within the nanoparticle, and 30% was measured in the supernatant as released insulin. During the period from 30 to 120 min, less than 50% of the initial insulin is detectable in either the supernantant or as retained within the particle, suggesting that acid degradation of insulin is taking place. It appears that some portion of the insulin is being chemically degraded, whether inside or outside of the nanoparticles.

It is likely that the insulin is being hydrolyzed due to the acidic environment of the simulated gastric fluid (pH 1.2). This degradation in acid has been reported previously and is pronounced at body temperature (37°C). Insulin is susceptible to deamidation in acidic solutions, especially at the A21 asparagine[78] [79]. This deamidation produces monodesamidoinsulin and a free carboxylic acid[80]. The hydrolyzed insulin is unresponsive to ELISA so it is not detected.

Additionally, the release profile in the gastric fluid shown in Figure 29 is different from that in Figure 28. Figure 28 indicates that no insulin release occurs in gastric fluid, but results in Figure 29 show that 30% of the insulin is released. The differences are possibly due to the differences in analytical methods for insulin quantification. HPLC was used to generate the data in Figure 28 while ELISA was used for the data in Figure 29. ELISA is a more sensitive technique that is able to detect very small quantities of insulin. It is possible that the amount released in gastric fluid is below the detection limit of HPLC.

4.2.3 Adjusted Microbead Model

The adjusted microbead model is based on the concept of producing microbeads, but replicating the polymer complexity and structure of the nanoparticle system. The formulation components are the same as the nanoparticle model but the method of preparation of the bead core is based on external gelation of alginate in calcium chloride, as was used in the original microbead model discussed in section 4.2.1, followed by coatings of chitosan and BSA. Different concentrations of the components in the core

were investigated as well as varying concentrations of calcium chloride and extrusion rate used in forming the beads. **Table 7** depicts the experimental design used to choose the best formulation for this adjusted model.

Table 7. Optimization of adjusted microbead model

Extrusion Rate (mL/min)	Calcium Chloride Concentration (mM)	Alginate Concentration (% w/v)	Dextran Concentration (% w/v)	Poloxamer Concentration (% w/v)
0.125	18	0.063	0.039	0.037
0.125	18	2	1.24	1.17
0.125	100	0.063	0.039	0.037
0.125	100	2	1.24	1.17
0.25	18	0.063	0.039	0.037
0.25	18	2	1.24	1.17
0.25	100	0.063	0.039	0.037
0.25	100	2	1.24	1.17
0.5	18	0.063	0.039	0.037
0.5	18	2	1.24	1.17
0.5	100	0.063	0.039	0.037
0.5	100	2	1.24	1.17
1	18	0.063	0.039	0.037
1	18	2	1.24	1.17
1	100	0.063	0.039	0.037
1	100	2	1.24	1.17
2	18	0.063	0.039	0.037
2	100	0.063	0.039	0.037

The concentrations of alginate, dextran, and poloxamer within the core were varied as illustrated in the table, but the concentration ratios of the alginate, dextran, and poloxamer to one another were kept the same as that used for the nanoparticle model. The two sets of concentrations were chosen based on the levels of components used to formulate the microbead and nanoparticle systems. The low concentrations (0.063% alginate, 0.039% dextran, 0.037% poloxamer) were based on the nanoparticle model and

the higher concentrations (2% alginate, 1.24% dextran, 1.17% poloxamer) were based on the microbead system. Discrete, stable beads could not be formed using the low concentration solution as there was not enough polymer available. Beads could be formulated at the higher polymer concentrations for all extrusion rates and calcium chloride concentrations. Images of the resulting beads are displayed in **Figure 30** and **Figure 31**.

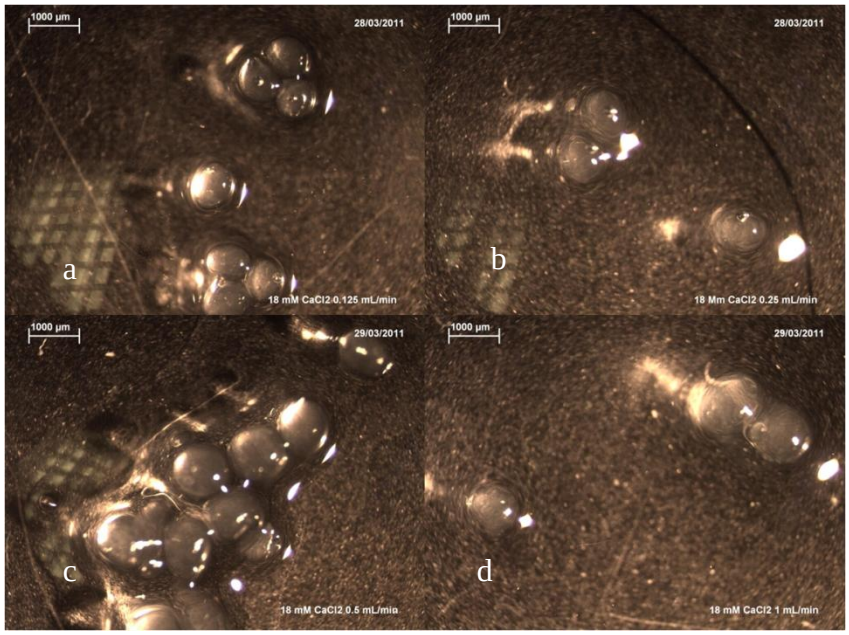

Figure 30. Adjusted microbead model prepared with 18 mM $CaCl_2$ at varying extrusion rates: (a) 0.125 mL/min (b) 0.25 mL/min (c) 0.5 mL/min (d) 1 mL/min

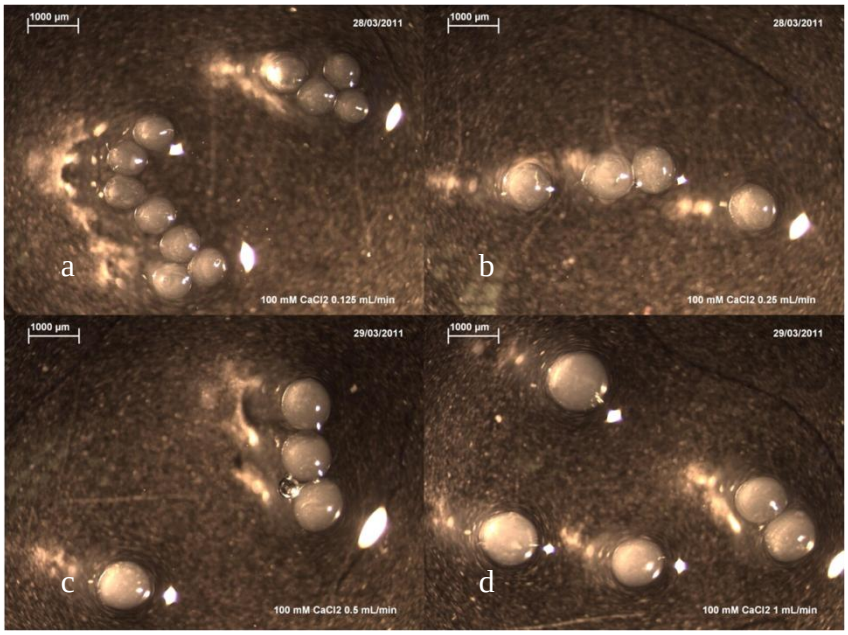

Figure 31. Adjusted microbead model prepared in 100 mM $CaCl_2$ at varying extrusion rates: (a) 0.125 mL/min (b) 0.25 mL/min (c) 0.5 mL/min (d) 1 mL/min

The beads were evaluated visually based on size, shape, and uniformity. It was the goal to produce small, spherical beads with minimum variation in size. It is evident that the beads formed in 100 mM calcium chloride are more spherical and uniform in size when compared to those formed in 18 mM calcium chloride. Also, as the extrusion rate was increased, the size of the beads increased slightly as well. Therefore, the optimal formulation was determined to be 2% alginate, 1.24% dextran, and 1.17% poloxamer extruded at 0.125 mL/min into 100 mM calcium chloride.

This core formulation was coated with 0.04% chitosan followed by 0.5% BSA solutions. After the last coating, a sample of beads was dissolved and the released insulin assayed with ELISA. Insulin loading was 0.20 ± 0.04 mg insulin/g particles. The stability and release kinetics of this new model were evaluated through measuring the release profile in simulated gastric and intestinal fluids. Samples of beads were tested

separately to evaluate behavior in gastric and intestinal conditions. Beads (0.5 g) were suspended in 10 mL of gastric or intestinal fluid for 2 h. Supernatant samples were taken over the course of the release period. ELISA was used to measure insulin release in gastric fluid and FITC-insulin measured to quantify release in intestinal fluid. The use of ELISA was necessary for the gastric release due to insulin degradation observed in this fluid. Quantification of label present would not be able to detect this degradation since the label is present even if the insulin has been broken down. No degradation was observed in intestinal fluid so FITC-insulin was a valid analytical method for these conditions.

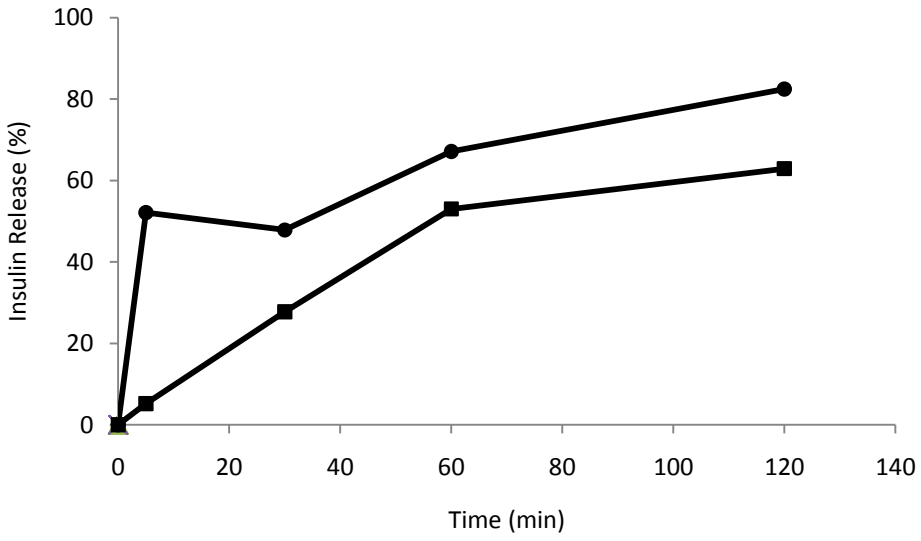

Figure 32. Gastric (■) and intestinal (●) release profiles for adjusted microbead model

In **Figure 32**, it is seen that 60% of the encapsulated insulin is released after 2 hours in gastric simulation, suggesting that 40% of the insulin is retained due to bead compaction in acidic gastric fluid. This was confirmed by dissolving the beads in 0.1 M PBS and 0.1

M EDTA after the 2 h gastric release where the remaining 40% of the insulin was found retained within the beads showing that all insulin is accounted for. Unlike the nanoparticles, all of the insulin is accounted for, thus there is no apparent hydrolysis of the insulin. One possible reason is that the alginate could have a protective effect against the acid, preventing insulin degradation. The adjusted microbeads contain a larger amount of alginate compared to the nanoparticles, and the amount of beads used in the release fluid (500 mg) is much higher than the nanoparticles (10 mg), increasing the alginate concentration further.

A higher level of release compared to the gastric release profile occurs under the neutral conditions of the intestinal fluid. Almost 50% of the insulin is released shortly after the beads are exposed to the intestinal fluid. At the end of 2h, 80% of the initial insulin was released into the supernatant. This intestinal profile is similar to those associated with the microbeads and nanoparticles shown in Figure 12 and Figure 28, since close to all insulin is eventually released once the beads or particles are exposed to intestinal conditions. One notable difference is the amount released during the first few minutes of exposure to intestinal fluid. In this release experiment, the beads were not exposed to gastric fluid before being transferred to intestinal fluid, which is what was done in the previous experiments. Prior exposure to acid would cause the beads to collapse reducing the amount released when transferred to neutral pH medium. Beads that were not first exposed to acid released a greater amount of insulin during the first few minutes in intestinal fluid than those that were exposed to acid. Only 10% was initially released for beads with prior exposure to gastric fluid as shown in Figure 12. This is compared to 52% release after five minutes in intestinal fluid in this experiment.

More insulin was released under gastric conditions compared to the microbeads and nanoparticles but the amount released was still less than what was released in intestinal fluid.

Sizing analysis was performed for this delivery model to evaluate the behavior of beads in simulated gastric and intestinal fluids. Bead diameter was measured in a BSA solution to determine the size of the beads after formulation. The beads were stored in a 0.5% BSA solution since BSA is the last coating applied before use or storage. Then, 2.5 g of beads were rinsed several times with simulated gastric fluid before being added to 100 mL of gastric fluid, then agitated for 1 h before size measurements were taken. The effect of intestinal fluid was evaluated by rinsing the beads and then mixing them in 100 mL of intestinal fluid for 1 h before measurements were taken. The results are shown in **Figure 33**.

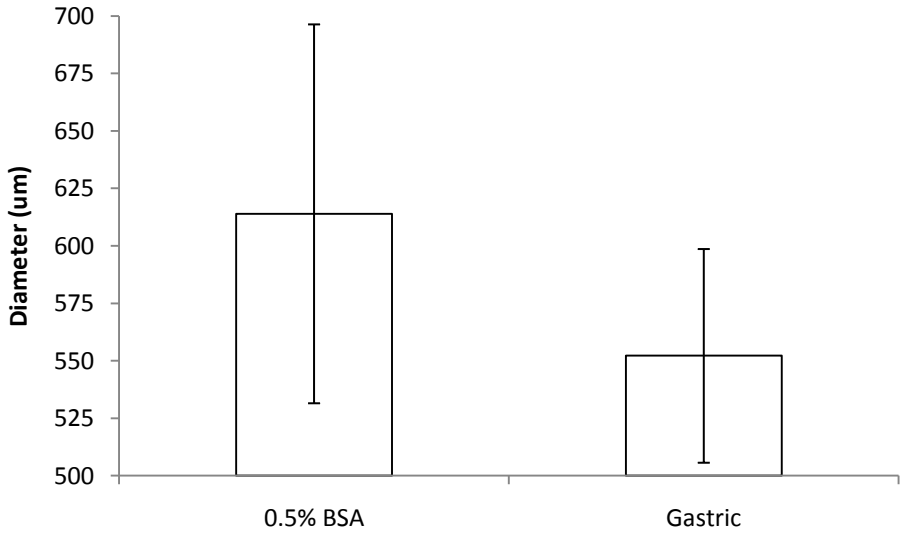

Figure 33. Size analysis of adjusted microbeads in 0.5% BSA solution and gastric fluid (no data shown for intestinal fluid as beads dissolved after 1 h mixing period)

The average diameter of the beads in 0.5% BSA solution is 613.9 ± 82.4, and the average diameter after 1 h in gastric fluid is 552.2 ± 46.5. No size was determined in intestinal fluid since all beads had dissolved after the 1 h mixing period. The average volume of the beads initially is 0.121 mm^3 and the average volume in gastric fluid is 0.088 mm^3. These results are similar to those in Figure 23 where there is a noticeable decrease in bead volume when transferred from storage solution in gastric fluid, where the ratio of the volumes in gastric fluid to the initial diameter is 73%. The gastric fluid thus causes the beads to collapse resulting in a smaller average diameter.

4.3 Evaluation of GI Simulators

4.3.1 Mixing Patterns

Two GI simulators were evaluated for *in vitro* testing of insulin delivery devices. One is an actively mixed simulator which is made up of a small flask and stir bar agitated at 100 rpm. The other is a passively mixed simulator consisting of a Tedlar bag mounted on a Roto-Shake Genie at 10 cycles per minute. The GI simulators were first evaluated based on the mixing time which is expected to affect insulin release. The mixing patterns were determined by tracking the decrease in pH caused by an addition of acid tracer. Results comparing the actively mixed simulator, and passively mixed simulator operating in either a rocking or rotating motion are shown in **Figure 34**.

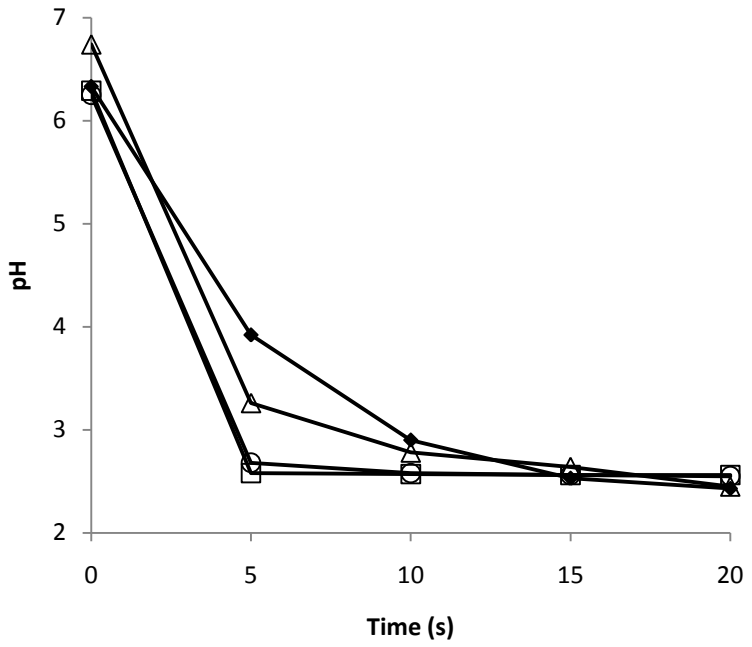

Figure 34. Mixing patterns for testing of insulin release under GI simulation: probe response (□), actively mixed simulator (○), rotating passively mixed simulator (Δ), rocking passively mixed simulator (♦)

The probe response was measured by transferring the probe from a magnetically stirred flask containing water to another flask containing water and added HCl making the change in pH conditions instantaneous. The plotted response then indicates the response rate of the pH probe. The mixing behavior of the actively mixed simulator closely follows the probe response. It is likely that the mixing pattern of the actively mixed simulator is faster than indicated here and thus measurement is limited by the probe response. The mixing times for the passively mixed simulator are slower than both the probe response and actively mixed simulator as indicated by the longer time required for the pH to stabilize.

The differences in the mixing patterns can also be demonstrated through the evaluation of the time constants for mixing. The time constant is defined as the time to

reach 63.2% of maximum pH response. Time constants were calculated based on plots of measured proton concentration. An example for the actively mixed simulator is represented in **Figure 35**.

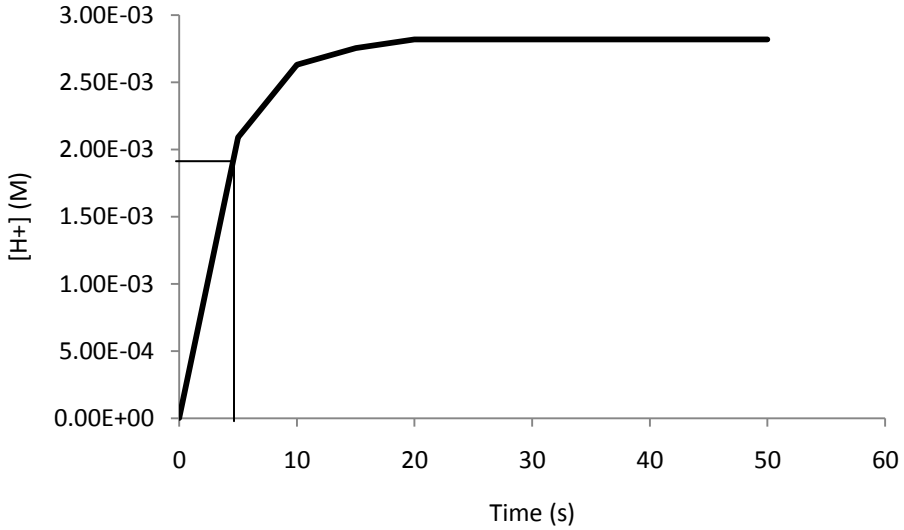

Figure 35. Time constant evaluation for actively mixed simulator

The time constant for the probe response was 3.8 s. It is assumed that the time constant for the actively mixed simulator is then equal to or less than 3.8 s. The time constant for mixing is 13.8 s for the rocking passively mixed simulator and 31.3 s for the rotating passively mixed simulator. The longer mixing times and higher values of the time constants demonstrate that the passively mixed simulator provides mixing that is gentler than the actively mixed system. The passively mixed simulator is more representative of the mixing behavior seen along the GIT. Peristaltic contractions in the stomach can occur for just a few minutes or several hours depending on the size and consistency of the meal[53]. Therefore, the time constant for mixing in the stomach is likely to be much

higher than the 31.8 s measured with the rocking passively mixed simulator. This indicates that the passively mixed simulator still provides a mixing behavior which is more active than physiological conditions in the GIT, but it is an improvement over the actively mixed simulator.

4.3.2 Evaluation of Simulators with Microbead Model

The GI simulators were evaluated through a release study using the microbead drug delivery model system to determine differences in release profiles using these different mixing methods. The microbeads were tested in the actively mixed simulator and passively mixed simulator using the rocking attachment. In both the actively mixed and rocking passively mixed simulator, the microbeads were subjected to gastric conditions (pH 1.7) for 60 min, then intestinal conditions (pH 7.4) for 100 min. Supernantant samples were analyzed using a Micro-BCA assay. The results are represented in **Figure 36**.

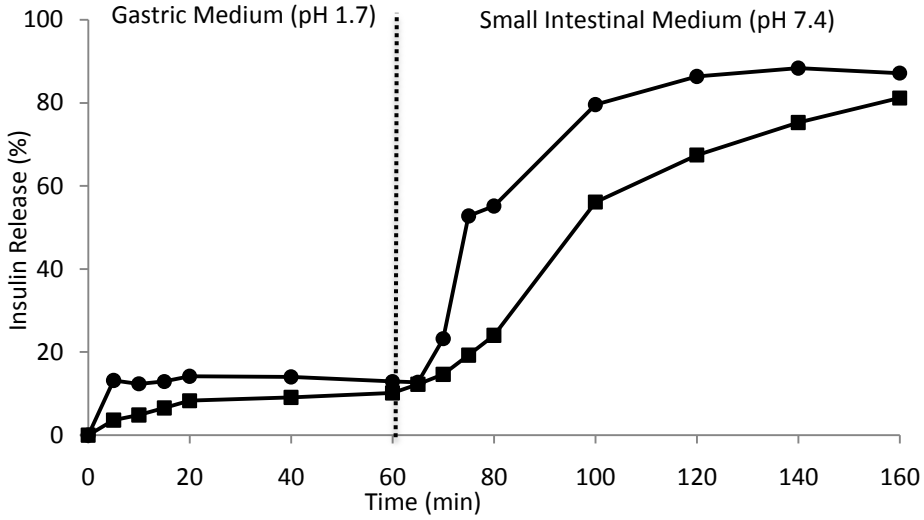

Figure 36. Simulator comparison with microbeads: rocking passively mixed simulator (■), actively mixed simulator (●)

Both GI simulators result in a similar overall pattern of release kinetics for insulin from microbeads. Under gastric conditions, a small release of insulin was observed within the first few minutes, but beyond that point, there is no apparent further release. This result could also be due to insulin being degraded by the acid as was discussed with the nanoparticle model in section 4.2.4, however since almost all of the insulin is released in the intestinal fluid, acid hydrolysis does not seem to be a factor in this case. This is similar to the result for the adjusted microbeads where the presence of alginate in the gastric fluid protects the insulin from hydrolysis. The microbeads are thought to collapse in acidic pH due to the protonation and resulting precipitation of alginate polymer which makes up the bead structure. The collapsed bead would then become less permeable, retaining insulin. The initial release would occur during the early transient period of particle collapse, expelling water and with it, some of the entrapped insulin. Once the

beads have fully collapsed, remaining insulin is then trapped within the bead[74]. Once the microbeads are transferred to the neutral intestinal fluid, the balance of the insulin is released. During this period under simulated intestinal conditions, the microbeads swell allowing the insulin to pass through the more openly permeable bead. For the actively mixed simulator, all of the insulin is released after 120 min while only 65% of the insulin was released for the rocking passively mixed simulator. At the end of the 160 min, insulin was still not fully released in the rocking passively mixed simulator.

Time constants for insulin release were evaluated for both systems under gastric and intestinal conditions. In gastric fluid, the time constant is 2 min for the actively mixed system and 12 min for the rocking passively mixed system. For the intestinal fluid, the time constant is 20 min for the actively mixed simulator and 40 min for the rocking passively mixed simulator. This indicates that a longer mixing time is required to achieve maximum insulin release from the microbeads using the rocking passively mixed simulator as compared to the actively mixed simulator under gastric and intestinal conditions. These results are similar to those in section 4.3.1, indicating that mixing behavior affects insulin release *in vitro* and thus must be taken into account when extrapolating results to *in vivo* conditions. *In vitro* mixing conditions that more closely mimic those in the GIT would promote better retention of insulin in the delivery device.

4.3.3 Evaluation of Simulators with Nanoparticle Model

The simulators were then evaluated with the insulin-loaded nanoparticles, for both the actively mixed and rocking passively mixed simulator. Insulin was measured in

supernatant samples using ELISA. Insulin release profiles for gastric and intestinal simulations are shown in **Figure 37**.

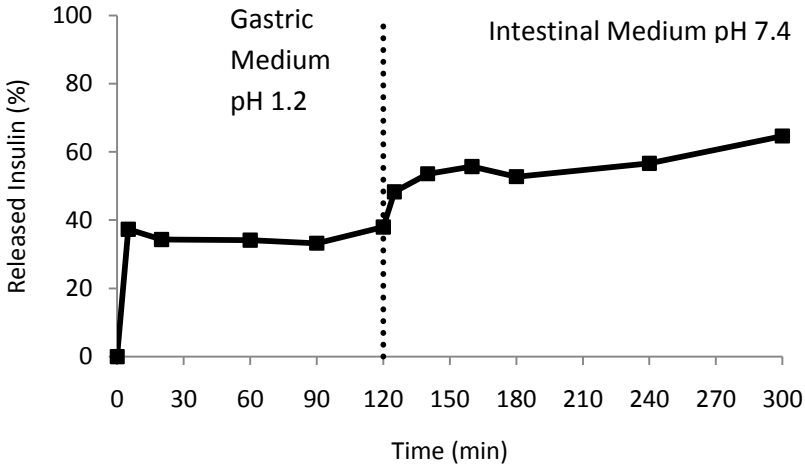

Figure 37. Insulin release from nanoparticles in rocking passively mixed simulator

These results can be directly compared to Figure 28 which was performed in an actively mixed simulator[44]. During the first two hours under gastric conditions, no insulin release was detected in the actively mixed simulator and 35% was released in the rocking passively mixed simulator. The particles become more impermeable in acid, thus retaining most of the insulin. In Figure 28, most of the insulin is released under intestinal conditions where the particles swell in neutral pH, resulting in a more permeable polymer matrix. The most significant difference in the results between the actively mixed and rocking passively mixed simulator occur during the three hour exposure to simulated intestinal fluid. After 180 minutes, 100% of the insulin is released in the actively mixed simulator while only 53% is released in the rocking passively mixed simulator. Another notable difference is the analytical method used to quantify insulin. In Figure 28 the insulin was measured using HPLC but in this study insulin was measured with ELISA

which is more sensitive than HPLC so some of the differences in the data could be attributed to the method of insulin quantification. These results are similar to what was seen in Figure 35 with the microbead model, with more insulin release detected for the actively mixed simulator which is more vigorously mixed.

4.3.4 Evaluation of Simulators with Adjusted Microbead Model

Release studies were performed with the adjusted microbeads in the actively mixed and rocking passively mixed simulators. In the actively mixed simulator, beads (0.5 g) were added to 10 mL of simulated gastric fluid without enzyme (USP31-NF26). In the rocking passively mixed simulator, 2.5 g were suspended in 50 mL of simulated gastric fluid without enzymes (USP31-NF26). Supernatant samples were taken for 2 h and insulin was quantified with ELISA. Results comparing the two simulators are shown in **Figure 38**.

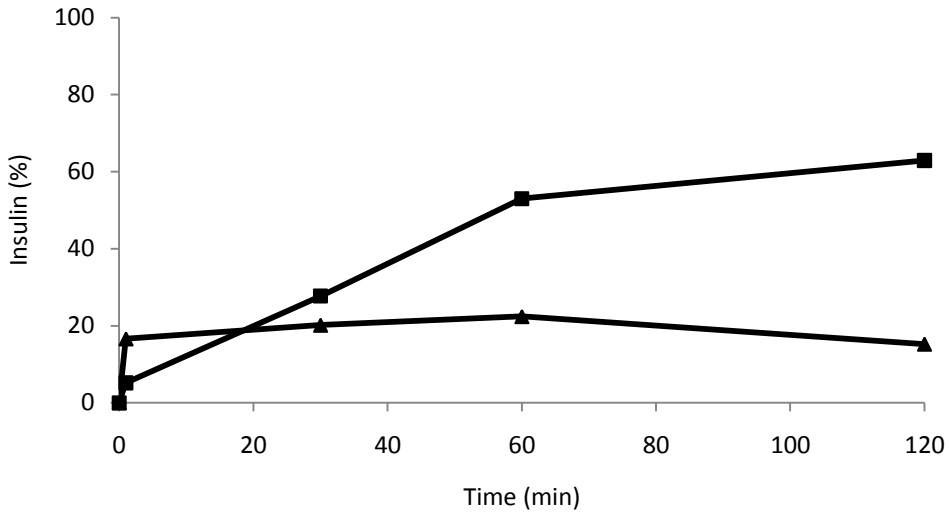

Figure 38. Insulin release from adjusted microbeads in simulated gastric fluid without enzymes: actively mixed (■), rocking passively mixed (▲)

The amount of insulin released in gastric conditions at the end of 2 h is less when using the rocking passively mixed simulator. Over 60% of the originally encapsulated insulin is released after 2 h in the actively mixed simulator while only 15% is released in the rocking passively mixed simulator. These results are similar to those obtained with the microbead model and nanoparticle model in Figures 36 and 37. The stronger mixing of the actively mixed simulator causes a greater release of insulin. The gentler mixing of the rocking passively mixed simulator allows more of the insulin to be retained within the beads, translating to more available insulin when the beads enter the small intestine.

The results of the release studies for both the microbead and nanoparticle models show that the type of simulator, or agitation method, plays an important role in the release characteristics seen under simulated GI conditions. More vigorous mixing techniques will promote a larger release of insulin from the drug delivery device at a faster rate. The rocking passively mixed simulator proved to be a better representation of

in vivo conditions than the actively mixed simulator since it allowed a slower release of insulin, indicating the way a drug delivery device is handled will directly impact release behavior as it passes through the GI tract. Mixing in the stomach can last between just minutes and several hours indicating that the stomach can be a poorly mixed environment. The passively mixed simulator provides a more gently mixed environment compared to the actively mixed simulator. Therefore, it is important to give careful consideration to agitation techniques used for *in vitro* models, especially when predicting drug delivery device behavior in the GI tract.

4.4 Simulation in Presence of Gastrointestinal Enzymes

The simulated gastrointestinal fluid was the other component of the GI model that was investigated, focusing especially on the effect of enzymes. Proteases in the stomach and intestines will break down insulin as it would any other ingested protein. Pepsin is the main protease in the stomach, while trypsin, chymotrypsin and other carboxypeptidases are the most important proteases in the small intestine[48]. The focus of this investigation was on the effects of the intestinal enzyme trypsin and gastric enzyme pepsin on the ability of a delivery device to protect insulin from degradation.

4.4.1 Effect of Trypsin on Insulin Encapsulated in Nanoparticles

Trypsin was chosen as a representative intestinal enzyme to test insulin susceptibility to digestion and the degree of protection provided by the nanoparticles. Initially, it was important to determine if insulin hydrolyzed by trypsin would be immunoresponsive to

ELISA antibodies. Insulin in Tris buffer was exposed to trypsin for different time periods. The ratio of the molar concentration of insulin was equal to that of trypsin. Trypsin was inhibited with trypsin inhibitor from Glycine max (soybean), a serine protease inhibitor, before ELISA analysis. The mass concentration of trypsin was equal to that of the trypsin inhibitor as recommended by the supplier (Sigma-Aldrich)[68]. Controls of Tris buffer alone and Tris buffer with trypsin and inhibitor were run to confirm that there was no assay interference with the buffer or the trypsin and inhibitor. **Table 8** provides the experimental design for this study.

Table 8. Experimental design for trypsin degradation of free insulin

	Incubation Time at 37°C (h)	Tris (mL)	3.5×10^{-4} mg/mL Insulin (mL)	0.06 μM Trypsin (mL)	0.072 μM Inhibitor (mL)
Tris Buffer	24	15	0	0	0
Trypsin with Inhibitor	24	5	0	5	5
Insulin no Trypsin 1	1	10	5	0	0
Insulin with Trypsin 1	1	0	5	5	5*
Insulin no Trypsin 2	2	10	5	0	0
Insulin with Trypsin 2	2	0	5	5	5*

*Inhibitor solution added after incubation time and mixed for 30 min at 37°C before ELISA

No interference was observed for the controls. Insulin in Tris buffer without trypsin was compared to insulin that was exposed to trypsin for different time periods through detection with a human insulin ELISA. The results comparing these scenarios are shown in **Figure 39**.

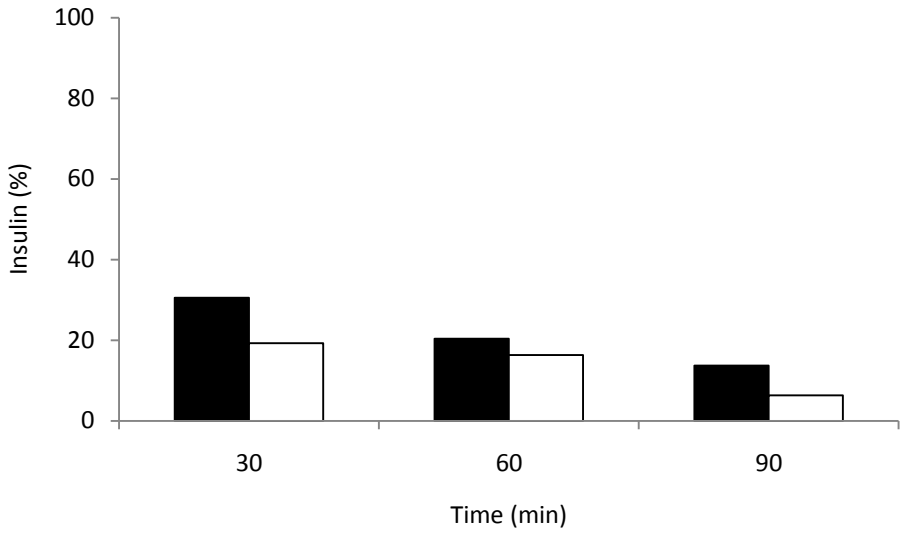

Figure 39. ELISA measurable insulin after exposure to trypsin at 37°C: insulin without trypsin (■), insulin with trypsin (□)

These results show that insulin is being lost whether it is or is not exposed to trypsin. There is a decrease in the amount of insulin present after trypsin exposure at each time point compared to the samples in intestinal fluid without enzyme, but it is not large enough to truly evaluate the effects of trypsin on insulin. The loss of insulin in samples not exposed to trypsin is likely due to instability at elevated temperature since the experiment was performed at body temperature (37°C). Insulin released from delivery systems at room temperature did not show this instability since high amounts of insulin were detected in the supernatant (65-87%) during release studies performed in simulated intestinal fluid without trypsin as shown in Figures 22, 32, 36 and 37. The plasma half-life of insulin in the body is 4 to 6 min[11], showing that insulin is cleared rapidly from the bloodstream. Therefore, it is possible that insulin is highly unstable under conditions that are more similar to those in vivo.

The effectiveness of the nanoparticle polymer matrix in protecting encapsulated insulin from protease degradation was evaluated using trypsin in Tris buffer at neutral pH. Exposed nanoparticles were treated with inhibitor at sample points then dissolved. ELISA detectable insulin was measured to determine the amount of insulin retained within the nanoparticles at 1, 2, or 5 h. At each time point, less than 1% of the original insulin was found intact within the particles. This is due to the fact that most of the insulin is released from the nanoparticles into the trypsin solution. This large release was seen previously in Figure 28 where 100% release of insulin is achieved after 60 min in intestinal fluid. It is likely that more insulin was retained at time points less than one hour and would have allowed for a better analysis on the effects of trypsin on the encapsulated insulin. This would have provided greater insight into the protective nature of the nanoparticle system.

4.4.2 Pepsin Degradation of Insulin

Pepsin was applied to study the adjusted microbeads and determine if the bead structure provides protection from enzymatic degradation under gastric conditions. Beads tend to retain more insulin in gastric fluid than those exposed to neutral intestinal conditions as discussed in section 4.2.3. If more insulin remains inside the particle, the effectiveness of the beads in protecting the insulin can be examined. In addition, acid hydrolysis was not as prevalent for this model compared to the nanoparticles as was discussed in section 4.2.3.

As with the trypsin investigation, pepsin was tested with insulin to examine the kinetics of insulin proteolytic hydrolysis. Pepsin cleaves proteins at the aromatic amino

acid residues Phe, Trp, and Tyr[81]. The hydrolysis reaction was stopped with pepstatin A as pepsin inhibitor prior to insulin assay using ELISA.

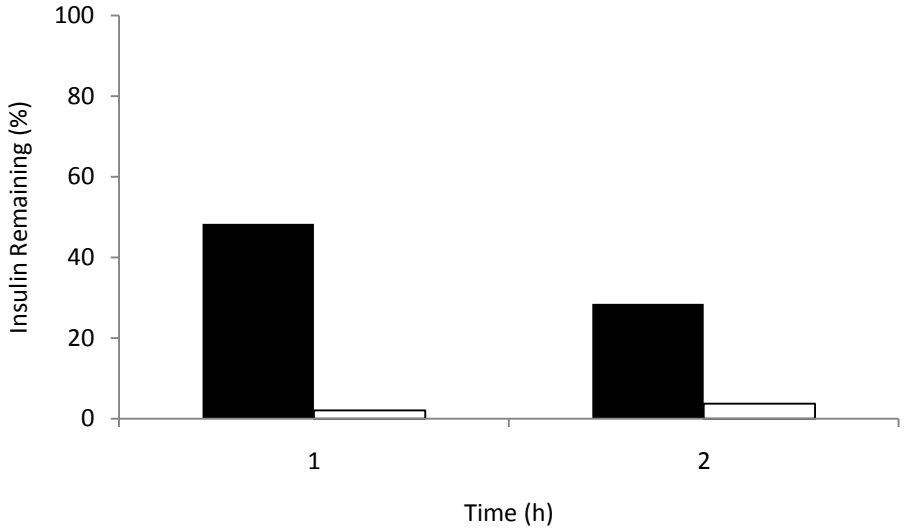

Figure 40. Degradation of insulin by pepsin at 37°C: insulin no pepsin (■), insulin with pepsin (□)

Results plotted in **Figure 40** indicate that insulin is fully degraded after 1h in pepsin solution. Additionally, insulin is lost due to contact with the acidic gastric fluid, likely due to acid hydrolysis which was described previously in section 4.2.2 and Figure 29 or degradation due to temperature sensitivity as discussed in section 4.4.1 and Figure 39. For both the nanoparticles and adjusted microbeads, at least 50% of the insulin was not detectable after exposure to gastric conditions at body temperature for 1 or 2 h.

The adjusted microbead model was then applied to determine if the polymer matrix would be able to protect retained insulin from pepsin degradation at body temperature. Beads were exposed to gastric fluid with pepsin and results were compared to those

exposed to gastric fluid without enzyme. A third batch involved beads exposed to enzyme free gastric medium for 30 min before addition of pepsin to allow time for beads to compact before pepsin exposure. Pepsin was inhibited through the addition of pepstatin A in ethanol before ELISA. At the end of the experiment, all bead samples were dissolved to determine the amount of ELISA detectable retained insulin. Results are shown in **Figure 41**.

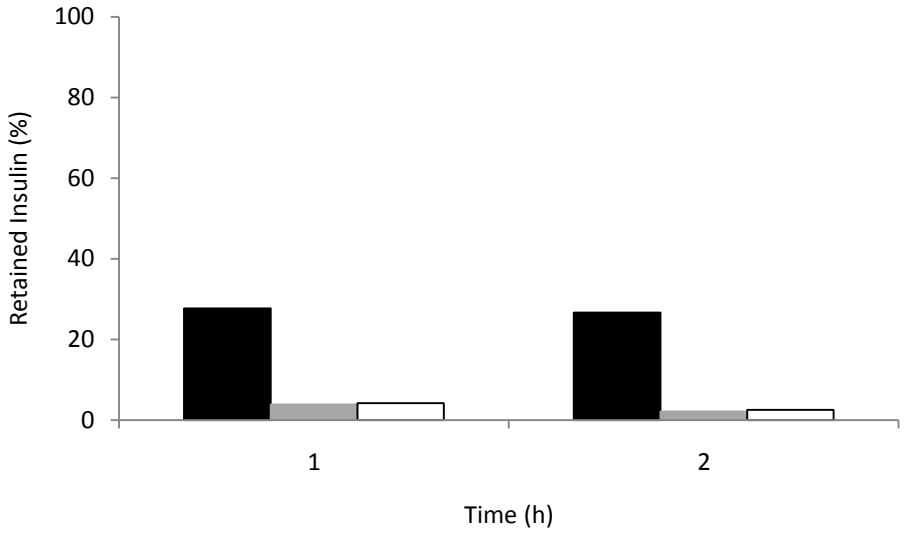

Figure 41. Effect of pepsin on insulin in adjusted microbead model: beads in gastric medium without pepsin (■), beads in gastric medium with pepsin (■), and beads in gastric medium without pepsin for 30 min before pepsin addition (□)

Under enzyme free gastric conditions at body temperature, 70% of the insulin was lost by 1h, and in the presence of pepsin, there was little residual intact insulin. Pepsin does play a role in degradation, as less than 5% of the insulin remains after enzyme exposure.

Pepsin degradation of insulin was compared between the two GI simulators. Adjusted microbeads were exposed to gastric fluid with pepsin and results were compared to those

exposed to gastric fluid without pepsin. Beads (2.5 g) were added to 50 mL of fluid, and agitated for 1 or 2 h before the addition of pepstatin A inhibitor. Beads were dissolved in a solution of 0.1 M PBS and 0.1 M EDTA, and released insulin quantified with ELISA. The results are summarized in **Figure 42**.

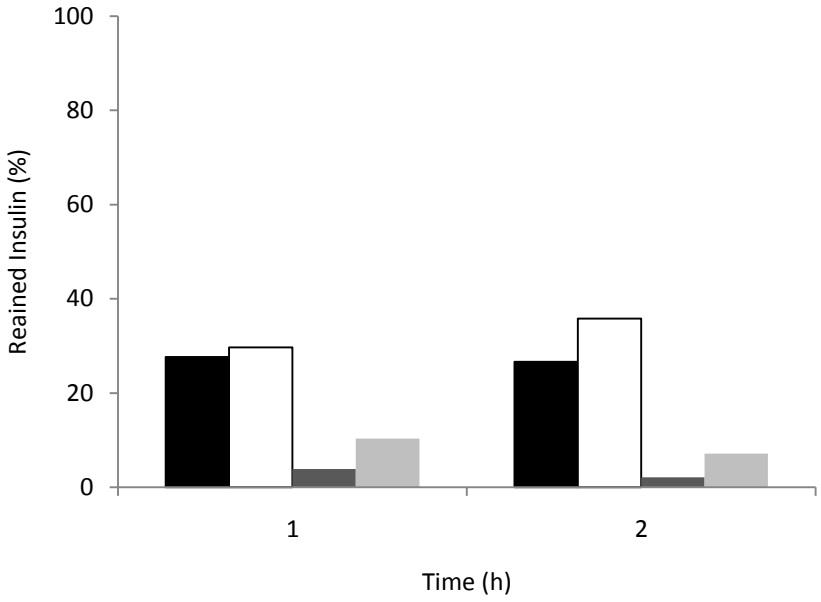

Figure 42. Insulin retained in adjusted microbeads in gastric fluid with and without pepsin in GI simulators at 37°C: actively mixed simulator no pepsin (■), rocking passively mixed simulator no pepsin (□), actively mixed simulator with pepsin (■), rocking passively mixed simulator with pepsin (■).

The results comparing insulin retained with and without pepsin are similar to those in the previous figure where a large portion of the insulin is broken down when exposed to pepsin and is unable to be detected by the ELISA. This is seen for both the actively mixed and rocking passively mixed simulators, but there is a slight improvement to insulin retained for the rocking passively mixed simulator. For a 1 h exposure to pepsin,

insulin retention is increased from 4% in the actively mixed system to 10% in the rocking passively mixed system. For a 2 h exposure, insulin retention is improved from 2% in the actively mixed system to 7% in the rocking passively mixed system. While these differences may be small, they indicate that mixing has an impact on how delivery devices will behave in simulated GIT fluids. Stronger mixing promotes more insulin release, exposing it directly to the GIT environment where acid hydrolysis and degradation by pepsin and high temperatures can easily occur. Coatings for alginate microbeads were examined in a previous study[82]. BSA was one of the coating materials evaluated for its ability to protect insulin. The BSA coated beads were able to retain 5% of the encapsulated insulin after exposure to gastric fluid with pepsin which is similar to the 10% or less retained in this experiment. These results suggest that the chitosan and BSA coatings do not provide significant protection to the encapsulated insulin. It is possible that the coating solutions applied were too low in concentration so the resulting coatings on the beads were not sufficient to protect insulin and limit its release from the polymer matrix in comparison to the nanoparticle model.

Previous researchers conducted testing with pepsin to evaluate the molecular integrity of particle systems. In one study, insulin was encapsulated in nanospheres with an alginate/dextran core coated with chitosan-polyethylene glycol and albumin[46]. After exposure to pepsin, the remaining insulin in the nanospheres was quantified with HPLC analysis and all insulin was accounted for. This indicates that the nanospheres were able to protect the insulin from pepsin degradation, which is contradictory to the results achieved in this study with the adjusted microbeads. Woitiski et al. (2010)[44] tested the nanoparticle formulation used here for insulin protection from pepsin[44]. After pepsin

exposure, 82% of the encapsulated insulin was detected by HPLC. These results contradict what was concluded here since the nanoparticles were able to protect most of the insulin from enzyme degradation. As mentioned previously, the difference in analytical methods (HPLC versus ELISA) could account for the different results. ELISA can detect much smaller quantities of insulin compared to HPLC so any changes in insulin concentration will be better detected when evaluated with ELISA. In addition, ELISA will only detect fully intact and thus bioactive insulin, while the UV detector on the HPLC analysis will not be so specific.

4.5 Simulated Intestinal Buffers

Different simulated intestinal buffers without enzyme were studied to determine effects on insulin release. Three formulations were tested: standard phosphate buffer, standard Kreb's bicarbonate buffer, and Kreb's bicarbonate buffer with a 1:1 NaCl:$CaCl_2$ ratio. Adjusted microbeads (2.5 g) were added to 50 mL of buffer in the rotating passively mixed simulator. Supernatant was sampled for 150 minutes and was analyzed with ELISA. The results are shown in **Figure 43**.

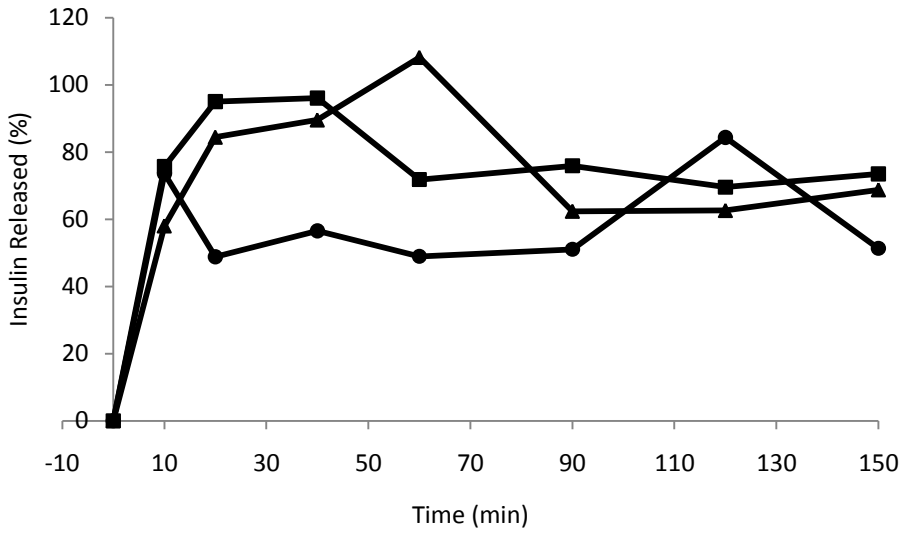

Figure 43. Insulin release from adjusted microbeads in standard phosphate buffer (■), standard Kreb's bicarbonate buffer (▲), and Kreb's bicarbonate buffer with 1:1 NaCl:$CaCl_2$(●)

The insulin release profiles for standard phosphate buffer and Kreb's bicarbonate buffer are similar in that 85 – 95% of the insulin is released in 20 minutes. Less insulin release was observed in the alternate Kreb's bicarbonate buffer where only 48% was released after 20 minutes, likely due to the stabilizing effect of the calcium. Fluctuations in the release profiles were observed likely due to the complex interactions between the insulin and its environment, including charge interactions that could affect the movement of insulin in and out of the microbeads. Additionally, the tertiary structure of the insulin may be altered which could potentially alter the responsiveness of the ELISA. These results demonstrate that the type of buffer used to simulate intestinal conditions will affect the behavior of the drug delivery device. The components in the simulated intestinal buffer can interact with the components of the delivery system, influencing the resulting insulin release profile.

4.6 Implication of GI Conditions on Stability of Insulin

Insulin is very unstable in GI fluid under various conditions. Acid hydrolysis can occur in gastric fluid. The beads are not able to protect the insulin, and degradation occurs whether or not the insulin is inside the bead or released into the medium. Additionally, enzyme degradation, especially pepsin, can break down significant amounts of insulin. Temperature can also have an effect on insulin functionality, where degradation can occur rapidly at body temperature. This indicates that acid hydrolysis, enzymatic degradation, temperature degradation and premature release of insulin from the encapsulation system are significant challenges in oral delivery.

These are major obstacles for oral insulin delivery and pose great challenges when designing an effective delivery device. Different studies on methods to orally deliver insulin have shown that insulin is protected from degradation to different degrees. It is important for insulin to be protected from gastric conditions so it can be successfully transported to the small intestine. In the small intestine, insulin can be released at absorption sites along the intestinal mucosa where uptake can occur. Additionally, insulin delivery can be achieved by uptake of the delivery device directly if it is small enough. The microbeads and adjusted microbeads were more effective at protecting insulin from acid hydrolysis in gastric fluid as compared to the nanoparticles. This was thought to be due to greater amounts of alginate present causing a protective effect in the gastric fluid, thus preserving the insulin and its intrinsic properties. The small size of the nanoparticles is necessary in order to encourage particle and thus insulin absorption

across the intestinal barrier. All of these components impact the pharmacological availability of insulin during *in vivo* studies. *In vivo* studies with the nanoparticles resulted in 11% availability[44] while a study using nanospheres showed greater availability of 42%[46]. Values between 10 and 20% can be considered adequate when evaluating the performance of a delivery device[47]. In the case of the nanoparticles, most of the insulin is lost or damaged in the GIT, indicating that this delivery system is not able to fully protect insulin from the many complex and harsh conditions in the GIT. The nanospheres provide better protection to the insulin as suggested by higher availability. The components of the nanospheres are very similar to the nanoparticles but the formulation techniques are very different. The goal of future research would then be to develop a delivery system through material choice and preparation method that is better able to promote bioactive insulin uptake in the small intestine while protecting it from the numerous factors that can cause insulin degradation.

Chapter 5: Conclusions and Future Recommendations

Diabetes is a serious disease with continuously increasing prevalence around the world. Insulin therapy is the most common treatment and is administered through subcutaneous injection. This method of delivery causes a number of problems associated with negative side effects and poor patient compliance. One method of overcoming this is with oral insulin delivery which is better able to mimic the effects of physiological insulin in addition to improving patient quality of life. Many different devices have been developed so it is imperative to have reliable methods to evaluate their effectiveness.

The overall goal of this study was to develop a simple GIT simulator to be used for routine *in vitro* testing of oral insulin delivery devices. The simulator was developed to mimic the technique and intensity of mixing observed in the GIT and was referred to as a passively mixed simulator. This was compared to an actively mixed simulator involving a magnetically stirred flask which is a commonly applied technique. Additionally, the effects of intestinal enzymes were investigated, specifically trypsin and pepsin. Different delivery devices were evaluated to determine their effectiveness in protecting against enzymatic degradation of insulin.

Three different delivery devices were used to evaluate the simulators: a microbead model, a nanoparticle model, and an adjusted microbead model. Different insulin quantification methods were applied depending on what was most appropriate for the situation: Micro-BCA assay, human insulin ELISA, and FITC fluorescence. Microbeads are alginate beads formed by extruding alginate droplets under an air jet into a calcium crosslinking solution. Beads have a size range of 700 – 1000 μm. Insulin is loaded into

the beads in two different ways. The first method involves incorporating the insulin into the alginate solution before gelation. The resulting beads had an insulin loading of 0.11 mg insulin/g beads. During a release study, the beads released 15% of the encapsulated insulin under gastric conditions and released the remaining insulin once they were transferred to intestinal conditions. Beads collapse under acidic conditions and prevent insulin release. In neutral intestinal fluid, beads will swell and allow greater insulin release. Insulin was also loaded through absorption into fully formed alginate beads. Insulin had a preference to the alginate compared to the insulin solution due to charge effects. Greater release in gastric fluid was observed compared to the beads loaded with insulin before gelation. It is thought that this is due to more insulin near the surface of the bead allowing for a greater initial release.

The nanoparticle model is a previously developed formulation that consists of insulin with a core of alginate, dextran, and poloxamer formed by ionotropic gelation[66]. This core is then coated with chitosan and BSA through polyelectrolyte complexation. The coatings are added to prevent premature insulin release and protect the insulin from degradation by acid and enzymes. The range of diameters in nanoparticle batches is 400 – 600 nm. The average insulin loading is 3.9 mg insulin/g particles. The results of a previously reported release study showed no release in gastric fluid and 100% release after exposure to intestinal fluids[44].

The adjusted microbead model was developed to analyze the formulation components of the nanoparticle model while avoiding some of the handling complications by producing larger beads. The optimal formulation consists of 2% alginate, 1.24% dextran, and 1.17% poloxamer added drop wise under an air jet into 100 mM calcium chloride at a

rate of 0.125 mL/min. Coatings of chitosan and BSA are applied to mimic those used in the nanoparticle system. The average insulin loading was determined to be 0.2 mg insulin/g beads. Release studies were performed in gastric and intestinal fluids separately where 60% of the insulin was released after 2 hours in gastric fluid compared to 80% released after 2 hours in intestinal fluid.

The actively mixed and passively mixed simulators were compared through a number of different investigations. The actively mixed simulator is a magnetically stirred flask system agitated at 100 rpm. The passively mixed simulator is a flexible bag that is rocked back and forth at 10 cycles per minute. The simulators were first compared through a pH tracer experiment where it was found that slower mixing occurred in the passively mixed simulator than was demonstrated by a larger time constant for mixing compared to the actively mixed simulator. It is likely that mixing is still too vigorous in the passively mixed system when compared to physiological conditions in the GIT where stomach contractions can last for minutes or hours depending on the type and quantity of meal ingested.

The simulators were also compared by performing release studies with the three insulin drug delivery models. The release with the microbeads showed slower insulin release for the passively mixed simulator in both gastric and intestinal conditions. In addition, longer time constants in gastric and intestinal fluids were calculated for the passively mixed simulator as compared to the actively mixed simulator indicating that the passively mixed simulator produces gentler mixing. Similar differences were seen with the release profiles using the nanoparticles. In the actively mixed simulator, 100% of insulin was released after 1 h in intestinal fluid while only 53% was released in the

passively mixed simulator at this same time point. Finally, the simulators were evaluated using the adjusted microbeads in gastric fluid for 2 h. At the end of the experiment, 60% of insulin was released in the actively mixed simulator and 15% was released in the passively mixed simulator. The results with all of the delivery models suggest that insulin release is greater under more intense mixing conditions. It is clear that the actively mixed simulator induces greater mixing as seen by the larger release of insulin compared to the passively mixed simulator.

The effects of gastrointestinal enzymes were then evaluated using pepsin in the gastric fluid and trypsin in the intestinal fluid. The nanoparticles and adjusted microbeads were applied to determine their abilities to protect insulin from enzymatic degradation. The nanoparticles were used to characterize the effects of trypsin, but insulin was released so rapidly that an effective evaluation of trypsin effects was not possible. This indicates that premature release of insulin in intestinal fluid is a larger issue than possible degradation by trypsin.

The adjusted microbeads were used to determine the effects of pepsin on encapsulated insulin. In the actively mixed simulator, there was a 95% loss of insulin when beads were exposed to pepsin in gastric fluid but there was also a 70% loss when beads were exposed to gastric fluid without enzyme. This indicates that significant a significant amount of insulin is released into the simulated gastric fluid. The adjusted microbeads were also tested in the passively mixed simulator with pepsin. Slight improvements in insulin retention were observed in the passively mixed simulator. After 1 hour pepsin exposure, insulin retained was increased from 4% in the actively mixed simulator to 10% in the passively mixed simulator. After 2 hours, insulin retention was increased from 2%

to 7%. These results indicate that pepsin degradation of insulin is a significant issue for oral insulin devices, but results vary depending on the type of mixing applied. Similar results were achieved in a study using BSA to coat alginate microbeads[82]. After pepsin exposure, only 5% of the insulin was detected. Different results were achieved with two other studies looking at the effects of pepsin on nanospheres and nanoparticles[44 46]. In both cases, 100% of the insulin was accounted for after exposure to pepsin. These discrepancies are likely due to differences in analytical techniques used to quantify intact insulin present.

Various buffers were evaluated as simulated intestinal fluids. Insulin release from the adjusted microbeads in standard phosphate buffer, standard Kreb's bicarbonate buffer, and Kreb's bicarbonate buffer with a 1:1 ratio of NaCl:$CaCl_2$ was compared. From 85-95% insulin release was observed after 20 min in the standard phosphate and Kreb's bicarbonate buffers, while only 48% was released in the Kreb's buffer with 1:1 NaCl:$CaCl_2$. This is likely due to the stabilizing effect of the higher calcium concentration which aids the beads in retaining more insulin. These results indicate that buffer choice for the simulated intestinal fluid will influence the kinetics of insulin release from the oral delivery system.

Mixing techniques affect the way a drug delivery device will behave during *in vitro* testing. From this study, it was shown that more vigorous mixing promotes more insulin release. A system with gentler mixing allows more insulin to stay encapsulated within the device and avoid direct contact with the GIT. The passively mixed simulator developed in this study is still more active than the mixing conditions seen in the GIT but it is an improvement over the actively mixed simulator commonly applied with *in vitro*

release testing. Gastrointestinal fluid and enzymes also affect the behavior of insulin devices. The effects of trypsin were not able to be determined since premature insulin release prevented observation of differences between samples with or without enzyme. Pepsin caused noticeable degradation of insulin in addition to the acid hydrolysis that was observed in the gastric fluid and was especially pronounced in the actively mixed simulator.

Oral insulin delivery has great potential as a replacement for subcutaneous insulin injections used for treatment of diabetes. Many obstacles still exist that have prevented this technology from being commercially available, some of which were observed throughout this study. Significant amounts of insulin are lost in the GIT as indicated previously by low values for pharmacological availability (11 – 42%)[44 46]. The insulin that is not accounted for is likely lost due to some of the obstacles discussed here. Premature insulin release from the delivery device exposes insulin directly to the harsh environment of the GIT and prevents it from effectively regulating blood glucose levels. Additionally, acid hydrolysis, temperature denaturation, and enzymatic degradation will further decrease the amount of available insulin. A successful oral insulin delivery method will be able to address all of these challenges so insulin can be pharmacologically effective in managing blood glucose levels in diabetic patients.

Future work on this topic relates to improvements to the oral insulin drug delivery device as well as the *in vitro* model used for evaluations. In regard to the delivery device, better protective coatings could be investigated since insulin breakdown is a significant barrier to oral delivery. Additionally, other protective techniques could be investigated that would protect the insulin whether or not it is encapsulated within the device. This

would be important if the insulin is released prematurely and may increase the amount of pharmacologically available insulin present. Other work relates to improvements of the *in vitro* model. Currently, the passively mixed system does not incorporate temperature control which plays a significant role in insulin stability. Additionally, more complex simulated gastrointestinal fluids could be incorporated to better mimic the complex environment of the GIT. While making these improvements, it is always necessary to achieve a balance between complexity and ease of use so that is still possible to perform routine testing with the more complicated model.

References

1 Zimmet, P. (2000). Globalization, Coca-colonization and the Chronic Disease Epidemic: Can the doomsday scenario be averted? *Internal Medicine in the 21st Centure*, 247, 301 – 310.

2 Finch, C. F., Zimmet, P. Z. (1988). Mortality from diabetes. *Alberti KGMMKrall LP. eds. The Diabetes Annual/4 Amsterdam*: Elsevier, 1-16.

3 Lipscombe, Lorraine L., Hux, Janet E. (2007). Trends in diabetes prevalence, incidence, and mortality in Ontario, Canada 1995-2005: a population-based study. *Lancet*, 369, 750 – 756.

4 Zimmet, P. Z. (1999). Diabetes epidemiology as a trigger to diabetes research. *Diabetologia*, 42, 499 – 518.

5 Canadian Diabetes Association. An economic tsunami, the cost of diabetes in Canada. Toronto, ON: Canadian Diabetes Association; 2009.

6 Raj, N.K. Kavitha, Sharma, Chandra P. (2003). Oral insulin - a perspective. *Journal of Biomaterials Applications*, 17, 183 – 196.

7 Reis, Catarina Pinto, Veiga, F., Ribeiro, A., Neufeld, Ronald J. (2009). Design innovation for insulin delivery systems. *The Bioartificial Pancreas and Other Biohybrid Therapies*, 557 – 585.

8 Gowthamarajan, K., Kulkarni, Giriraj T. (2003). Oral insulin – fact or fiction? Possibilities of achieving oral delivery for insulin. *Resonance*, 38 – 46.

9 Reis, Cataraina Pinto, Neufeld, Ronald J., Ribeiro António, Veiga, Francisco (2006). Nanoencapsulation II. Biomedical applications and current status of peptide and protein nanoparticulate delivery systems. *Nanomedicine: Nanotechnology, Biology, and Medicine 2*, 53 – 65.

10 Saffran, Murrey, Pansky, Ben, Budd, G. Colin, Williams, Frederick E. (1997). Insulin and the gastrointestinal tract. *Journal of Controlled Release*, 46, 89 – 98.

11 Duckworth, William C., Bennett, Robert G., Hamel, Frederick G. (1998). Insulin degradation: progress and potential. *Endocrine Reviews*, 19 (5), 608 – 624.

12 Cernea, S., Raz, I. (2006). Noninjectable methods of insulin administration. *Drugs of Today*, 42(6), 405 – 424.

13 Dubin, Cindy H. (2009). Proteins and peptides: dependent on advances in drug delivery? *Drug Delivery Technology*, 9 (3), 29 – 34.

14 Bernstein, Gerald (2008). Delivery of insulin to the buccal mucosa utilizing the RapidMist ™ system. *Informa healthcare*, 5 (9), 1047 – 1055.

15 Belanger, A. (2002). Efficacy and safety of inhaled insulin (Exubera((R))) compared to subcutaneous insulin therapy in patients with type 2 diabetes: results of a 6-month, randomised, comparative trial. *Diabetologia*, 45, A260 – A261.

16 Thayer, Ann M. (2010). Nicer than needles: delivering biologic drugs orally, instead of by injection, calls for tricking the human body. *Chemical and Engineering News*, 88 (22), 27 – 30.

17 Novo Nordisk starts phase 1 trial with oral insulin analogue. *Novo Nordisk Press Release,* 2009.

18Luzio, S. D., Dunseath, G., Lockett, A., Broke-Smith, T. P., New, R. R., Owens, D. R. (2009). The glucose lowering effect of an oral insulin (Capsulin) during an isoglycaemic clamp study in persons with type 2 diabetes. *Diabetes, Obesity and Metabolism: A Journal of Pharmacology and Therapeutics*, 12 (1), 82 – 87.

19 Agarwal, V., Khan, M. A. (2001). Current status of oral insulin delivery. *Pharmaceutical Technology*, 76 – 90.

20 Damgé, Christiane, Pinto Reis, Catarina, Maincent, Philippe (2008). Nanoparticle strategies for the oral delivery of insulin. *Informa healthcare*, 5(1), 45 – 68.

21 Jung, T., Kamm, W., Breitenbach, A., Kaiserling, E., Xiao, J. X., Kissel, T. (2000). Biodegradable nanoparticles for oral delivery of peptides: is there a role for polymers to affect mucosal uptake? *European Journal of Pharmaceutics and Biopharmaceutics*, 50, 147 – 160.

22 Morçöl, T., Nagappan, P., Nerenbaum, L., Mitchell, A., Bell, S. J. D. (2004). Calcium phosphate-PEG-insulin-casein (CAPIC) particles as oral delivery systems for insulin. *International Journal of Pharmaceutics*, 277, 91 – 97.

23 Reis, Catarina Pinto, Ribeiro, António J., Houng, Simone, Veiga, Francisco, Neufeld, Ronald J. (2007). Nanoparticulate delivery system for insulin: Design, characterization and in vitro/in vivo bioactivity. *European Journal of Pharmaceutical Sciences*, 30, 392 – 397.

24 Woitiski, Camile B., Carvalho, Rui A., Ribeiro, António J., Neufeld, Ronald J., Veiga, Francisco (2008) Strategies toward the improved oral delivery of insulin nanoparticles via gastrointestinal uptake and translocation. *Biodrugs*, 22 (4), 223 – 237.

25 Augst, Alexander D., Kong, Hyun Joon, Mooney, David J. (2006). Alginate hydrogels as biomaterials. *Macromolecular Bioscience*, 6, 623 – 633.

26 Orive, G., Carcaboso, A. M., Hernández, R. M., Gascón, A. R., Pedraz, J. L. (2005). Biocompatibility evaluation of different alginates and alginate-based microcapsules. *Biomacromolecules*, 6, 927 – 931.

27 Dang, Jiyoung M., Leong, Kam W. (2006). Natural polymers for gene delivery and tissue engineering. *Advanced Drug Delivery Reviews*, 58, 487 – 499.

28 Chan, Ariel W., Whitney, Ralph A., Neufeld, Ronald J. (2009). Synthesis of a controlled stimuli-responsive alginate hydrogel. *Biomacromolecules*, 10, 609 – 616.

29 Tønnesen, Hanne, Karlsen, Jan (2002). Alginate in drug delivery systems. *Drug development and Industrial Pharmacy*, 28 (6), 621 – 630.

30 Drury, Jeanie L., Dennis, Robert G., Mooney, David J. (2004). The tensile properties of alginate hydrogels. *Biomaterials*, 25, 3187–3199.

31 Poncelet, D., Lencki, R., Beaulieu, C., Halle, J. P., Neufeld, R. J., Fournier, A. (1992). Production of alginate beads by emulsification/internal gelation. I. Methodology. *Applied Microbiology and Biotechnology*, 38, 39 – 45.

32 Kierstan, M., Bucke, C. (1977). The immobilization of microbial cells, subcellular organelles, and enzymes in calcium alginate gels. *Biotechnology and Bioengineering*, 19, 387 – 397.

33 Vila, A., Sánchez, A., Tobío, M., Calvo, P., Alonso, M. J. (2001). Design of biodegradable particles for protein delivery. *Journal of Controlled Release*, 78, 15 – 24.

34 Dodane, Valérie, Amin Khan, M., Merwin, June R. (1999). Effect of chitosan on epithelial permeability and structure. *International Journal of Pharmaceutics*, 182, 21 – 32.

35 Abreu, Flávia O. M. S., Bianchini, Carla, Forte, Maria M. C., Kist, Tarso B. L. (2008). Influence of the composition and preparation method on the morphology and swelling behavior of alginate-chitosan hydrogels. *Carbohydrate Polymers*, 74, 283 – 289.

36 Illum, Lisbeth (1998). Chitosan and its uses as a pharmaceutical excipient. *Pharmaceutical Research*, 15 (9), 1326 – 1331.

37 Errington, N., Harding, S. E., Värun, K. M., Illum, L. (1993). Hydrodynamic characterization of chitosans varying in degree of acetylation. *International Journal of Biological Macromolecules*, 15, 113 – 117.

38 Hari, P. R., Chandy, Thomas, Sharma, Chandra P. (1996). Chitosan/calcium – alginate beads for oral delivery of insulin. *Journal of Applied Polymer Science*, 59, 1795 – 1801.

39 Ioan, Catalina E., Aberle, Thomas, Burchard, Walther (2000). Structure properties of dextran. 2. dilute solution. *Macromolecules*, 33, 5730 – 5739.

40 Sanford, P. A., Baird, J. (1983) Industrial utilization of polysaccharides. The Polysaccharides. Academic Press: 2, 474.

41 Reis, Catarina Pinto, Ribeiro, António, Veiga, Francisco, Neufeld, Ronald J., Damgé, Christiane (2008). Polyelectrolyte biomaterial interactions provide nanoparticulate carrier for oral insulin delivery. *Drug Delivery*, 15, 127 – 139.

42 Janes, Kevin A., Fresneau, Marie P., Marazuela, Ana, Fabra, Angels, Alonso, María José (2001). Chitosan nanoparticles as delivery systems for doxorubicin. *Journal of Controlled Release*, 73, 255 – 267.

43 Tiyaboonchai, Waree, Woiszwillo, James, Sims, Robert C., Middaugh, C. Russell (2003). Insulin containing polyethylenimine–dextran sulfate nanoparticles. *International Journal of Pharmaceutics*, 255, 139 – 151.

44 Woitiski, Camile B., Neufeld, Ronald J., Veiga, Francisco, Carvalho, Rui A., Figueiredo, Isabel V. (2010). Pharmacological effect of orally delivered insulin facilitated by multilayered stable nanoparticles. *European Journal of Pharmaceutical Sciences*, 41, 556 – 563.

45 S. Hirsjarvi, I. Peltonen, J. Hirvonen (2000). Surface pressure measurements in particle interaction and stability studies of poly(lactic acid) nanoparticles. *International Journal of Pharmaceutics*, 348, 153–160.

46 Reis, Catarina P., Veiga, Francisco J., Ribeiro, António J., Neufeld, Ronald J., Damgé, Christiane (2008). Nanoparticulate biopolymers deliver insulin orally eliciting pharmacological response. *Journal of Pharmaceutical Sciences*, 97 (12), 5290 – 5305.

47 Schilling, Robert J., Mitra, Ashim K. (1990). Intestinal mucosal transport of insulin. *International Journal of Pharmaceutics*, 62, 53 – 64.

48 Schulze, K. (2006). Imaging and Modelling of digestion in the stomach and duodenum. *Neurogastroenterol Motil*, 18, 172 – 183.

49 Kozu, Hiroyuki, Kobayashi, Isao, Nakajima, Mitsutoshi, Uemara, Kunihiko, Sato, Seigo, Ichikawa, Sosaku (2010). Analysis of flow phenomena in gastric contents induced by human gastric peristalsis using CFD. *Food Biophysics*, 5, 330 – 336.

50 Kong, F., Singh, R. P. (2008). Disintegration of solid foods in human stomach. *Journal of Food Science*, 73 (5), R67 – R80.

51 Bauer AJ, Publicover NG, Sanders KM (1985). Origin and spread of slow waves in canine gastric antral circular muscle. *Am J Physiol*, 249, G800.

52 Thomas, A. (2006). Gut motility, sphincters, and reflex control. *Anesthesia and Intensive Care Medicine*, 7 (2), 57 – 58.

53 Arnold, James G., Dubois, Andre (1983). *In vitro* studies of intragastric digestion. *Digestive Diseases and Science*, 28 (8), 737 – 741.

54 Hoebler, C., Karinthi, A., Devaux, M. F., Guillon, F., Gallant, D., Bouchet, B., Barry J. L. (1998). Physical and chemical transformations of cereal food during oral digestion in humans. *British Journal of Nutrition*, 80, 429 – 436.

55 Hoebler, C., Devaux, M. F., Karinthi, A., Belleville, C., Barry, J. L. (2000). Particle size of solid food after human mastication and *in vitro* simulation of oral breakdown.

56 Hoebler, C., Lecannu, G., Belleville, C., Devaux, M. F., Popineau, Y., Barry, J. L. (2002). Development of an *in vitro* system simulating bucco-gastric digestion to assess the physical and chemical changes of food. *International Journal of Food Sciences and Nutrition*, 53, 389 – 402.

57 Oomen, A. G., Rompelberg, C. J. M., Bruil, M. A., Dobbe, C. J. G., Pereboom, D. P. K. H., Sips, A. J. A. M. (2002). Development of an *in vitro* digestion model for estimating the bioaccessibility of soil contaminants. *Archives of Environmental Contamination and Toxicology*, 44, 281 – 287.

58 Versantvoort, Carolien H. M., Oomen, Agnes G., Van de Kamp, Erwin, Rompelberg, Cathy J. M., Sips, Adrienne J. A. M. (2005). Applicability of an *in vitro* digestion model in assessing the bioaccessibility of myotoxins from food. *Food and Chemical Toxicology*, 43, 31 – 40.

59 Molly, K., Woestyne, M. Vande, Verstraete, W. (1993). Development of a 5-step multi-chamber reactor as a simulation of the human intestinal microbial ecosystem. *Applied Microbiology and Biotechnology*, 39, 254 – 258.

60 De Boever, Patrick, Deplancke, Bart, Verstraete, Willy (2000). Fermentation by gut microbiota cultured in a simulator of the human intestinal microbial ecosystem is improved by supplementing a soygerm powder. *The Journal of Nutrition*, 130 (10), 2599 – 2606.

61 Minekus, M., Smeets-Peeters, M., Bernalier, A., Marol-Bonnin, S., Havenaar, R., Marteau, P., Alric, M., Fonty, G., Huis in't Veld, J. H. J. (1999). A computer-controlled system to simulate conditions of the large intestine with peristaltic mixing, water absorption and absorption of fermentation products. *Applied Microbiology and Biotechnology*, 53 (1) 108-114.

62 Minekus, M., Marteau, P., Havenaar, R., Huisintveld, J. H. J. (1995). A multicompartmental dynamic computer-controlled model simulating the stomach and small intestine. *Alternative to Laboratory Animals (ATLA) , 23* (2), 197-209.

63 Smith, P. K., Krohn, R. I., Hermanson, G. T., Mallia, A. K., Gartner, F. H., Provenzano, M. D., Fujimoto, E. K., Goeke, N. M., Olson, B. J., Klenk, D. C. (1985). Measurement of protein using bicinchoninic acid. *Analytical Biochemistry*, 150, 76 – 85.

64 Mercodia. (n.d.). *Principle of Technology*. Retrieved from http://www.mercodia.se/learning-center/mercodia-elisa-technology/principle-of-technology.html.

65 Clausen, Andreas E., Bernkop-Schnürch, Andreas (2001). Thiolated carboxymethylcellulose: in vitro evaluation of its permeation enhancing effect on peptide drugs. *European Journal of Pharmaceutics and Biopharmaceutics*, 51, 25 – 32.

66 Woitiski, Camile Baldin, Veiga, Francisco, Ribeiro, António, Neufeld, Ronald (2009). Design for optimization of nanoparticles integrating biomaterials for orally dosed insulin. *European Journal of Pharmaceutics and Biopharmaceutics*, 73, 25 – 33.

67 Schilling, Robert J., Mitra, Ashim K. (1991). Degradation of insulin by trypsin and alpha-chymotrypsin. *Pharmaceutical Research*, 8 (6), 721 – 727.

68 Sigma-Aldrich. "Trypsin inhibitor from Glycine max (soybean)." Retrieved from http://www.sigmaaldrich.com/canada-english.html.

69 Maeda, Hiroshi, Ishida, Nakao, Kawauchi, Hiroshi, Tuzimura, Katura (1969). Reaction of fluorescein isothiocyanate with proteins and amino acids. *The Journal of Biochemistry*, 65 (5), 777 – 783.

70 Gök, Elmas, Olgaz, Seda (2003). Binding of fluorescein isothiocyanate to insulin: a fluorimetric labeling study. *Journal of Fluorescence*, 14 (2), 203 – 206.

71 Lorenz, John N., Gruenstein, Eric (1999). A simple, nonradioactive method for evaluating single-nephron filtration rate using FITC-inulin. *American Journal of Physiology – Renal Physiology*, 276, F172 – F177.

72 Clausen, Andreas E., Bernkop-Schnürch, Andreas (2000). *In vitro* evaluation of the permeation-enhancing of thiolated polycarbophil. *Journal of Pharmaceutical Sciences*, 89 (10), 1253 – 1261.

73 Cheng, Sung-Ching, Wu, Yung-Chih, Mi, Fwu-Long, Lin, Yu-Hsin, Yu, Lin-Chien, Sung, Hsing-Wen (2004). A novel pH-sensitive hydrogel composed of N,O-carboxymethyl chitosan and alginate cross-linked by genipin for protein drug delivery . *Journal of Controlled Release*, 96, 285 – 300.

74 George, Meera, Abraham, T. Emilia (2006). Polyionic hydrocolloids for the intestinal delivery of protein drugs: alginate and chitosan — a review. *Journal of Controlled Release*, 114, 1 – 14.

75 Wintersteiner, Oskar, Abramson, Harold A. (1933). The isoelectric point of insulin. *Journal of Biological Chemistry*, 99 (3), 741 – 753.

76 Haug, Arne, Larsen, Bjørn, Smidsrød, Olav (1966). A study of the constitution of alginic acid by partial acid hydrolysis. *Acta Chemica Scandinavica*, 20, 183 – 190.

77 Malvern Instruments (2004). Zetasizer Nano Series User Manual. Worcestershire: Malvern Instruments Ltd.

78 Sundry, F. (1962). Separation and characterization of acid-induced insulin transformation products by paper electrophoresis in 7 M urea. *The Journal of Biological Chemistry*, 237 (11), 3406 – 3411.

79 Grau, U (1985). Chemical stability of insulin in a delivery system environment. *Diabetolgia*, 28, 459 – 463.

80 Geiger, Terrence, Clarket, Steven (1987). Deamidation, isomerization, and racemization at asparaginyl and aspartyl residues in peptides. *The Journal of Biological Chemistry*, 262 (2), 785 – 794.

81 Nelson, David L., Cox, Michael M. (2005). *Lehninger Principles of Biochemistry* (Fourth edition). New York: W. H. Freeman and Company.

82 Campbell, Adrienne, O'Brien, Lauren (2008). Formulation of an oral drug delivery system for insulin: protective coatings for microencapsulated insulin. *Queen's University Undergraduate Thesis.*